ENVIRONMENTAL ENGINEERING

EVALUATION OF THERMALLY ENHANCED SOIL VAPOR EXTRACTION USING ELECTRICAL RESISTANCE HEATING FOR CHLORINATED SOLVENT REMEDIATION IN THE VADOSE ZONE

ASHLEY HENDRICKS

Thesis under the direction of Professor David S. Kosson

Soil vapor extraction (SVE) is the most popular technology for removing volatile contaminants from the vadose zone. However, SVE is limited by the contaminant vapor pressure, hydraulic conductivity and gas permeability of the vadose stratigraphy. Concentration reductions greater than 90% are hard to achieve with traditional SVE. Thermal enhancement is establishing itself as a viable method to increase the applicability and effectiveness of SVE. Heating methods include steam injection, radiowave, microwave, and electrical resistance. The appropriate method depends on site geology, soil and contaminant parameters and the maximum temperature required. Electrical resistance heating (ERH) is one promising enhancement method. ERH has been demonstrated at more than 30 sites. However, little is known about the mechanisms occurring during the heating process. Existing models are limited in scope, neglecting important aspects of heat and mass transfer.

The purpose of the research presented is to develop the basis for a general mass transfer model to simulate the SVE process during remediation of chlorinated solvents using thermally enhanced SVE in the vadose zone. A conceptual model detailing the processes occurring during vapor extraction with soil heating by electrical resistance is proposed. The conceptual model is then used to derive a set of governing equations for a general multiphase multicomponent system with an applied heat flux. This approach allows the model developed here to be extended to other thermal treatments.

Approved:

David S. Kosson, Ph.D.

EVALUATION OF THERMALLY ENHANCED SOIL VAPOR EXTRACTION USING ELECTRICAL RESISTANCE HEATING FOR CHLORINATED SOLVENT REMEDIATION IN THE VADOSE ZONE

By

Ashley Hendricks

Thesis

Submitted to the Faculty of the

Graduate School of Vanderbilt University

in partial fulfillment of the requirements

for the degree of

MASTER OF SCIENCE

in

Environmental Engineering

May, 2006

Nashville, Tennessee

Approved:

David S. Kosson, Ph.D.
Florence Sanchez, Ph.D.
Christine Switzer, Ph.D.

ACKNOWLEDGEMENTS

This thesis was prepared with the support of the U.S. Department of Energy, under Award No. DE-FG01-03EW15336 to the Institute for Responsible Management, Consortium for Risk Evaluation with Stakeholder Participation II. However, any opinions, findings, conclusions, or recommendations expressed herein are those of the author and do not necessarily reflect the views of the DOE or of IRM/CRESP II.

I would especially like to thank Drs. Christine Switzer and David Kosson for their time, insights and putting up with me for nearly two years. Thanks are also in order for Nicole Comstock – bless anyone who tries to keep track of Dr. Kosson. Thank you also to Karen Page and Whitney Crouch for your support during my tenure at Vanderbilt.

Getting through my time at Vanderbilt would not have been possible without my two Amigos: Jennifer Miller (the soon to be Mrs. Williams) and Janey Smith. Long lunches and general ruckus-making would not have been as much fun without them. I must also thank the wonderful website gotradio.com for keeping me entertained and undistracted by the outside world.

I must acknowledge my parents, dear sister, Gretchen, and best friend, Athena. Without them nothing in life would be possible. I hope I have made you proud. Lucky, Sam and Shadow thank you so much for all your assistance with homework and typing. Your incessant distractions and wet noses keep me sane.

TABLE OF CONTENTS

LIST OF TABLES

Table **Page**

LIST OF FIGURES

Figures **Page**

NOMENCLATURE

Symbol		Units
A	Area	$[m^2]$
α	Phase (l, s, g)	
a	Surface a of control volume	
β	Component (TCE, water, soil, air)	
b	Surface b of control volume	
C_P	Specific heat at constant pressure	[J/kg-K]
C_v	Specific heat at constant volume	[J/kg-K]
c	Surface c of control volume	
CS	Control surface	
CV	Control volume	
d	Surface d of control volume	
e	Surface e of control volume	
F	Force	[N]
F_g	Force due to gravity	[N]
F_v	Viscous force	[N]
F_P	Force due to pressure	[N]
f	Surface f of control volume	
g	Acceleration of gravity	$[m/s^2]$
g	Gas phase	
h_{vap}	Heat of vaporization	[J/kg]
$\hat{H}$	Specific enthalpy	[J/kg]
H	Total enthalpy	[J/kg]
$\hat{H}_{vap}$	Heat of vaporization	[J/kg]
k	Thermal conductivity	[W/m-K]
l	Liquid phase	
m	Mass	[kg]
$\dot{m}$	Mass transfer rate	$[kg/m^3\text{-}s]$
M_w	Molecular weight	[g/mol]
n	Number of moles	[mol]
n	Normal vector	
η	Porosity	[-]

Symbol		Units
o	Initial	
θ	Moisture content	[-]
$\theta_{l,NAPL}$	Liquid NAPL content	[-]
$\theta_{l,water}$	Liquid water content	[-]
$\theta_{g,total}$	Total gas content	[-]
$\theta_{g,NAPL}$	Gaseous NAPL content	[-]
$\theta_{g,water}$	Gaseous water content	[-]
$\theta_{l,total}$	Total liquid content	[-]
φ	Space coordinate	
P	Pressure	[atm]
P_o	Initial pressure	[atm]
ρ	Density	[kg/m^3]
q	Heat flux	[W/m^2]
Q	Heat generation	[W/m^3]
r	Space coordinate	
r_w	Radius of SVE well	[m]
r_∞	Temperature far from the heated area	[K]
R_n	Radius of circular area (radius to electrode)	[m]
R	Universal Gas Constant	[J/mol-K]
ref	Reference state (i.e. temperature, pressure)	
S	Saturation	[-]
s	Solid phase	
sur	outer surface of circular area	
t	Time	[s]
T	Temperature	[K]
T_o	Ambient temperature (before heating)	[K]
T_{ref}	Reference temperature	[K]
T_{sur}	Temperature at the electrode area (outer surface of circular area)	[K]
$\hat{U}$	Specific internal energy	[J]
U	Total internal energy	[J]
v	Velocity	[m/s]
V	Volume	[m^3]
z	Space coordinate	

Symbol		Units
	Used by Others	
	STMVOC - Falta et al. (1992)	
Γ_l	Control Surface	
$\hat{C}_g^c$	Pseudo saturated vapor concentration	[kg/m^3]
$\bar{C}_g^c$	Saturated chemical vapor concentration	[kg/m^3]
C_{P_r}	Specific heat at constant pressure of rock grains	[J/kg-K]
$D_{i\beta}$	Diffusion coefficient tensor of component *i* in phase β	[m^2/s]
F^K	Total flux of component K	for K≠h: [kg/m^{2}s], for K=h: [J/m^{2}s]
K	Component (a=air, w=water, c=chemical, h=heat)	
κ	Diagonal intrinsic permeability tensor	[m^2]
M^K	Amount of component K per unit volume	for K≠h: [kg/m^3], for K=h: [J/m^3]
N	Outward unit normal vector	
q^K	Rate of generation of component K per unit volume	for K≠h: [kg/m^{3}s], for K=h: [J/m^{3}s]
S_β	Saturation of phase β	
S_n	NAPL saturation	[-]
V_l	Control Volume	
	Adenekan et al. (1993)	
$\mathbf{F}_i$	Molar flux of component *i* (*i*=1,…N)	[mols/m^{2}s]
g	Gravitational acceleration	[m/s^2]
g	Gas phase	
H_β	Molar enthalpy of the phases	[J/mol]
$k_{r\beta}$	Relative permeability of the phases	[cm^2]
λ	Effective thermal conductivity tensor	[W/m-K]
M_i	Molar weight of component *i*	[g/mol]
μ_β	Phase viscosity	[kg/m-s]
o	Oil (NAPL) phase	
φ	Porosity	[-]
P_β	Pressure in phase β	[atm]

Symbol		Units
ρ'_r	Mass density of rock grains	[kg/m^3]
ρ_β	Phase molar density	[mols/m^3]
ρ'_β	Mass density of phases	[kg/m^3]
q_i	Generation rate of *i* per unit volume of porous medium	[kg/m^3]
q_{heat}	Heat generation rate per unit volume	[J/m^3]
T	Temperature	[K]
t	Time	[s]
τ_β	Tortuosity of the flow of phase β	[-]
U_β	Molar internal energy of the phases	[J/mol]
w	Water phase	
w_{ir}	Adsorbed mass of component *i* per unit mass of rock grains	[kg/kg]
$x_{i\beta}$	Mole fraction of component *i* in phase β	[-]
	Buettner and Daily (1995)	
C	Specific heat	[J/kg-K]
k	Relative permeability	[m^2]
ρ	density	[kg/m^3]
T	Temperature	[K]
t	Time	[s]
	Benard et al. (2005)	
E	Internal energy per unit volume	[J/m^3]
g	Acceleration due to gravity	[m/s^2]
h_P	Enthalpy of phase *p* per unit mass	[J/kg]
ρ_P	Bulk density of phase *p*	[kg/m^3]
p	phase	
q	Conductive thermal flux	[W/m^2]
$\overline{Q}$	Heat source term	[W/m^3]
t	Time	[s]
$\mathbf{v}_P$	Specific flux of phase *p*	[m/s]

CHAPTER I

INTRODUCTION

1.1 Overview

Groundwater contamination by chlorinated solvents poses a serious threat to public health. In the 2002 Agency for Toxic Substances and Disease Registry (ASTDR) Annual Report, it was reported that more than 1.7 million people live within one mile of the 371 contaminated sites they studied. Volatile organic compounds (VOCs), including trichloroethylene (TCE), were found at approximately 20% of the sites assessed. TCE was most commonly used as an industrial degreaser for metal parts and was also used in typewriter correction fluids, paint removers, and adhesives (ASTDR, 2003). TCE is a probable human carcinogen with known acute and chronic central nervous system effects (United States Environmental Protection Agency [EPA], 2000).

Soil vapor extraction (SVE) is the most widely known and accepted method for vadose zone remediation at sites contaminated by TCE and other volatile chlorinated solvents. The proven performance of SVE and availability of equipment makes SVE an attractive remediation method for contamination in the vadose zone. However, concentration reductions of more than 90% are difficult to achieve and treatment times can range from six months to several years (EPA, 2000). Additionally, SVE can be used effectively only for contaminants with vapor pressures greater than 0.1 to 1.0 mm Hg at 20°C, hydraulic conductivities greater than $1x10^{-3}$ to $1x10^{-2}$ cm/s and Henry's Law constants greater than 100 atm per mole fraction (EPA, 1997).

Combining SVE with other technologies can extend the applicability of traditional SVE. Enhancements for SVE include as air sparging, dual phase extraction, hydraulic or pneumatic fracturing and thermal treatments (EPA, 1997). Thermal treatments include steam and hot air injection, radiowave, microwave, electrical resistance and thermal conduction heating. Heating the subsurface has two direct benefits: (1) increased vapor pressure of contaminants and (2) increased air permeability achieved through soil drying.

The inspiration of thermal SVE for remediation came from the petroleum industry's use of steam injection since the 1980s to recover petroleum products from subsurface formations. Other heating methods have been adapted from petroleum recovery approaches for application to thermally-enhanced SVE. Radiowave, microwave and electrical resistance have been used since the 1970s to extract bitumen from tar sand deposits (Acierno et al., 2003; Kawala and Atamanczuk, 1998). Thermal SVE has become popular in the past decade to reduce the time required for remediation, remove sorbed compounds with low vapor pressure, solubilize or vaporize non-aqueous phase liquids (NAPLs) and enhance biological activity (EPA, 1997).

1.2 Thesis Goals and Objectives

Although thermally-enhanced SVE has been studied for the past decade, very few studies have addressed heating technologies other than steam injection. Electrical resistance heating has been gaining momentum over the past few years as the preferred enhancement method for remediation in low permeability soils. The goal of this thesis is to formulate a general mass transfer model to simulate the SVE process augmented by electrical resistance heating. The specific objectives of this thesis are to:

- Develop a conceptual model detailing the processes occurring in the vadose zone during vapor extraction with soil heating by electrical resistance; and
- Use the conceptual model to develop a set of governing equations describing subsurface contaminant mass transfer during vapor extraction with soil heating by electrical resistance.

Specific tasks involved in addressing these objectives include: (1) developing a rubric to guide decisionmakers in selecting the most appropriate thermal enhancement for a given area, (2) deriving the appropriate multiphase equations for conservation of mass, momentum and energy, including representing heat flux due to evaporation and condensation processes, mass flux and convection and conduction processes, (3) contaminant mass transfer above the boiling point of the contaminant and water, (4) determining the appropriate simplifying assumptions.

CHAPTER II

LITERATURE REVIEW

2.1 Overview of Heating Techniques and Applications

The petroleum industry has been using subsurface thermal treatment for several decades as an enhanced oil recovery technique. Thermal recovery methods for *in-situ* recovery of oil are primarily used for viscosity reduction of the product (Dablow III et al., 2000; Chute and Vermeulen, 1988; EPA, 2004). Thermal enhancement by steam injection uses the injection pressures to mobilize petroleum products, such as crude oil, for extraction. However, heterogeneities within the reservoir may reduce the effectiveness of steam enhancement (Chute and Vermeulen, 1988). For this reason, electromagnetic heating has also been used as a thermal recovery method. Electromagnetic heating has been used to successfully extract bitumen from tar sand deposits (Acierno et al., 2003; Kawala and Atamanczuk, 1998). Radiofrequency heating has also been used to recover oil from oil shale with some success (Edelstein et al., 1994; Dwyer et al., 1979; Bridges et al., 1979; Dev et al., 1989).

The first implementation of steam heating for remediation occurred in the mid-1980s in the Netherlands (Dablow III et al., 2000). Steam injection in combination with soil vapor extraction (SVE) has been used extensively since that time as a thermal enhancement for subsurface remediation. Electrical resistance heating became commercially available in 1997 and has been demonstrated at more than 30 sites in the United States since 1999 (Beyke and Fleming, 2005). Radiofrequency heating was

successfully demonstrated at several sites beginning in the 1990s (Daniel et al., 1999). Microwave enhanced remediation has been verified as a plausible thermal enhancement in several lab-scale experiments to date (Kawala and Atamanczuk, 1998; Acierno et al., 2003; Di et al., 2002).

Contaminants that have vapor pressures of 10 mm Hg or greater in the temperature range required for remediation are suitable for electrical heating, including radiofrequency heating (RFH) (Sresty, 1994). For example, trichloroethylene (TCE) and tetrachloroethane (PCE) are both suitable for electrical heating while methylene chloride and 1,1-Dichloroethylene (1,1-DCE) are not due to their low vapor pressures even at increased temperatures. Figure 2-1 shows the relationship between vapor pressure and temperature for TCE, PCE, 1, 1-DCE and methylene chloride (CRC, 1990).

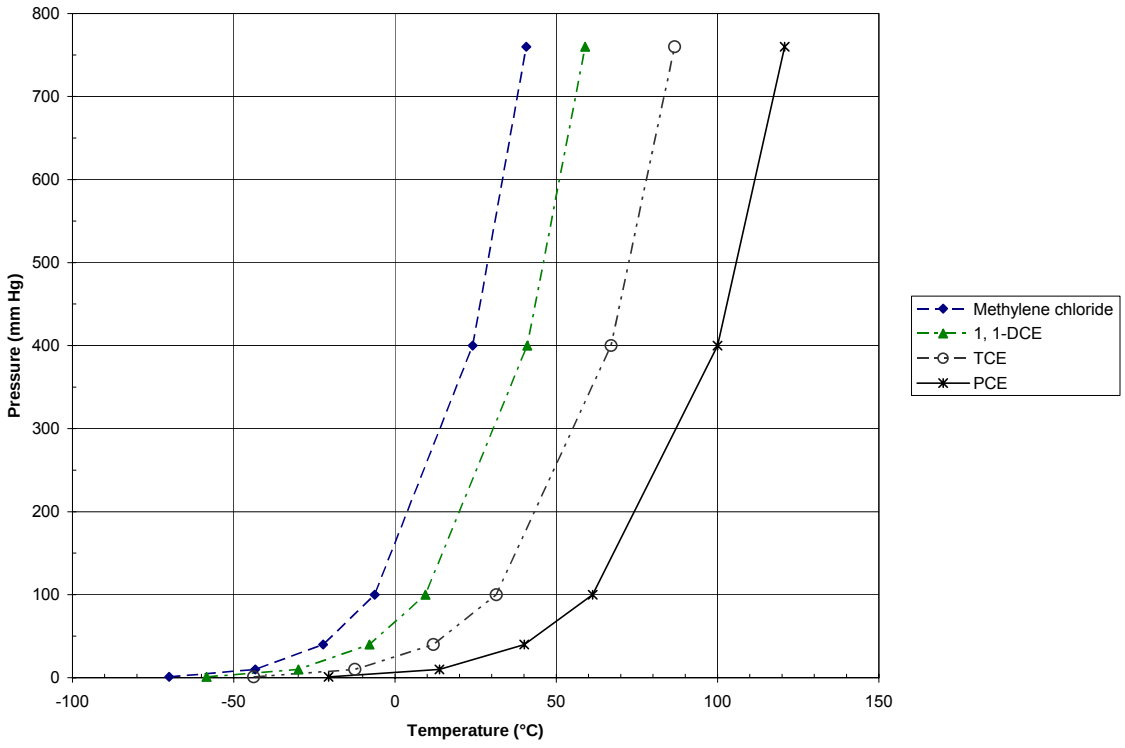

Figure 2-1: Vapor Pressure and Temperature for Selected Compounds

Contaminants with vapor pressures greater than 70 Pa at 25°C are applicable for remediation by soil vapor extraction based on prior field studies (Poppendieck et al, 1999). Vapor pressures of 70 Pa can be achieved at 150°C for up to 20 straight-chain carbons (Schwarzenbach et al., 1993; Poppendieck et al., 1999). Temperatures in the 150°C to 200°C range can extend the minimum vapor pressure requirement from 10 mm Hg to as low as 5 mm Hg (EPA, 1997).

2.1.1 Steam and Hot Air Injection

SVE enhanced with steam injection uses saturated steam at pressures high enough to penetrate the pores but low enough not to exceed the fracturing pressure (EPA, 2004). Fracturing can create channels for preferential flow where contaminated regions are not accessed. Depending on soil permeability, steam is injected at intervals from every few meters to more than ten meters (EPA, 2004; Davis, 1998).

Steam injected into a contaminated region enhances traditional SVE by driving contaminants toward vapor extraction wells (Figure 2-1). Steam forms when soil and pore fluids adjacent to the injection well reach the boiling point of water and the *in-situ* vapor pressure equals that of the sum of the fluid vapor pressures (EPA, 2004; Sleep and Ma, 1997). As the advancing edge of the steam front moves toward the extraction well, fluids including NAPLs are volatilized from the aqueous to vapor phase; resulting in a high concentration of vaporized contaminants behind the front (EPA, 2004).

Soils of moderate to high permeability, such as sands and gravels, are required for successful application of steam in the vadose zone. In addition, a layer of low permeability or confining layer below the contaminated zone is needed to prevent

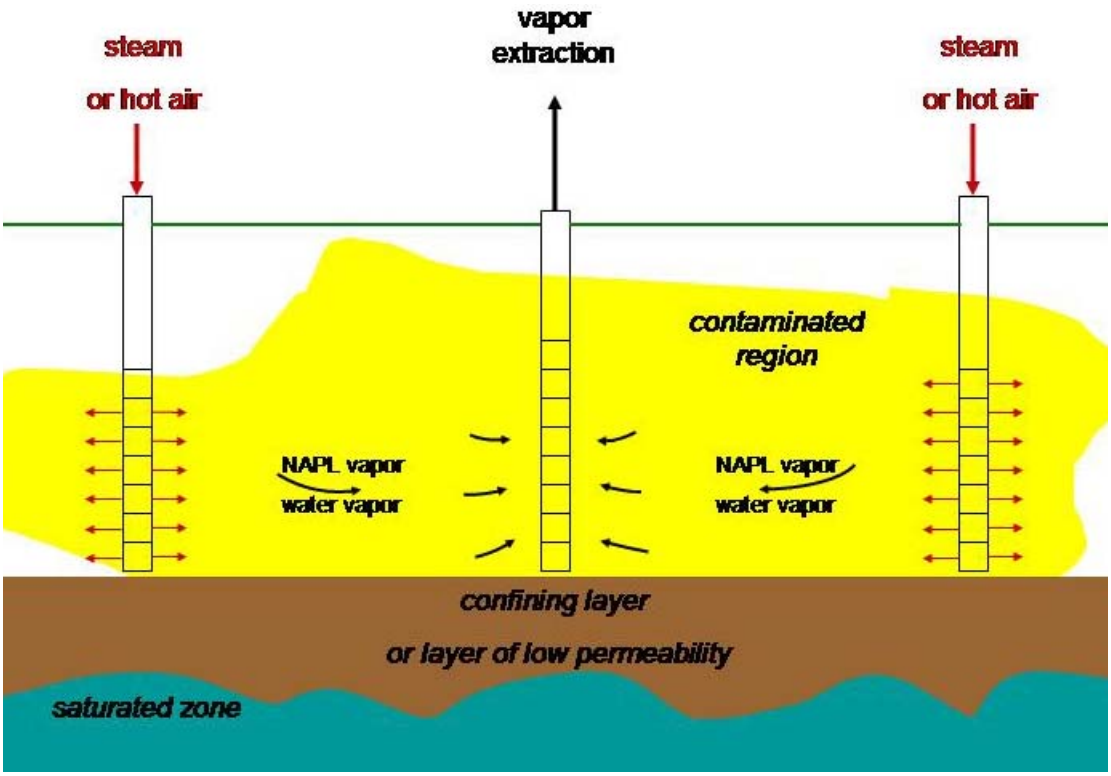

Figure 2-1: Steam Injection Schematic

downward contaminant migration to uncontaminated areas (EPA, 1997). Low permeability materials, such as clay-rich soils, do not allow the steam to move easily into the pores, resulting in ineffective heating (EPA, 1997).

Heterogeneities create a number of problematic conditions during steam flushing. Areas layered with impermeable and permeable regions may see the extent of contamination increased as the contaminants move along the permeable region (EPA, 1997). Preferential flow channeling around contaminated low-permeability regions of the subsurface is also a concern when heterogeneities are present (EPA, 1997; EPA, 2004).

Techniques that increase permeability, such as pneumatic fracturing, could be used in combination with steam injection to improve efficiency. Care must be taken with any permeability-enhancing technique to avoid remobilizing the contaminant downward to uncontaminated areas. Additionally, techniques for lower permeability regions, such as radiofrequency and electrical resistance heating, can also be used in combination with steam injection for targeted heating of low-permeability regions.

Hot air injection is similar to enhancement by steam injection but lower in cost. The heat capacity of air, however, is approximately four times less than that of steam, so higher flow rates are needed for hot air injection to achieve the same heating rate as steam injection. The vaporization/condensation process provides further heating in the steam injection process (EPA, 2004). Enhancement by hot air injection suffers the same stratigraphy limitations as steam injection.

2.1.2 Radio and Microwave Frequency

Radiofrequency heating (RFH) uses electrodes embedded in the soil to deliver electromagnetic energy which enhances SVE by increasing the vapor pressure of the contaminant, increasing soil permeability due to drying and decreasing viscosity. In a typical installation, electrodes are placed in rows of three, with two rows acting as ground electrodes. Electromagnetic energy is delivered to the third, which is placed between the ground rows (Van Deuren et al., 2002). One advantage to using RFH over other techniques is that this method is capable of heating soils to temperatures of at least 150°C to 200°C (Van Deuren et al., 2002; EPA, 1997). Temperatures of 300°C to 400°C are

believed to the upper range of achievable temperatures using RFH (Dev, 1993; Sresty, 1994) though temperatures in this range have not been demonstrated.

A RFH system consists of an RF generator, matching network, electrode/applicators, one or more antennae, temperature measuring devices, and an RF shield (EPA, 1997; Daniel et al. 1999). An RF generator transmits energy to the electrodes or antenna applicators (Price et al., 1999). Three phase alternating current power, which is commercially available from the local power utility in the United States, is converted into RF energy by a generator. A simple schematic of an RF enhanced soil vapor extraction system is shown in Figure 2-2.

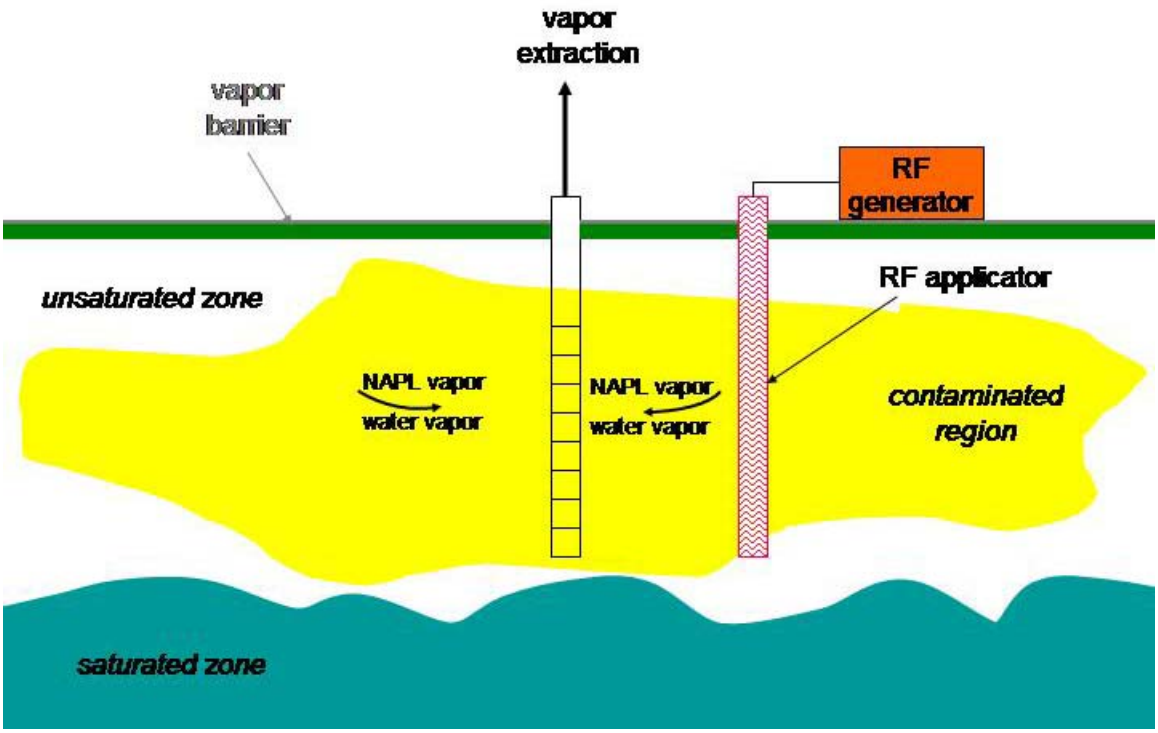

Figure 2-2: Radiofequency Heating Schematic

RF generators provide power, up to 25 kW, to a radiofrequency applicator which provides a continuous RF waves at several different frequencies approved, 6.78, 13.56, 27.12, or 40.68 Hz, for industrial, scientific and medical applications (EPA, 1997; Price et al., 1999). The frequency used is based on soil electrical properties, such as dielectric constant and electrical conductivity (Daniel et al., 1999; EPA, 1997; Price et al., 1999). The dielectric constant and the conductivity directly relate to the optimal wavelength and the soil's ability to absorb RF waves (Price et al., 1999). Matching networks modify the RF energy to maximize the efficiency of the power absorption based on soil properties (EPA, 1997). Energy is radiated into the soil by electrodes or antennae applicators. Thermocouples or other temperature measuring devices are placed in the soil to monitor heating. An RF shield may be needed if too much magnetic energy is escaping from the treatment area (EPA, 1997).

Managing proper moisture content is critical for RFH to be implemented effectively. Moisture is needed for radiofrequency waves to be absorbed by the soil. However, soils that are dry or become very dry during heating will cause the impedance to rise considerably and RF waves to not propagate sufficiently through the subsurface (Edelstein et al., 1994). Wet soils require significantly more RF energy to heat the soil to temperatures above 100°C (Daniel et al., 1999). Therefore, RFH has a greater potential than steam or hot water injection in low permeability soils such as clay; clay soils typically have higher water contents than other soils, allowing for more rapid heating and higher attainable temperatures (Davis, 1997).

Microwave heating is analogous to radiofrequency heating. Microwave heating uses electromagnetic waves with a wavelength of 1 mm to 1 m and a frequency between 300 MHz and 300 GHz; industrial and scientific applications typically use a frequency of 2.45 GHz (Acierno et al., 2003; Jones et al., 2002). Microwave induced steam distillation (MISD) has been studied by only a few authors (Di et al., 2002; Acierno et al., 2003; Kawala and Atamanczuk, 1998). Laboratory experiments have shown that heating is the most intense for polar substances, for which temperatures of 100°C are achievable (Kawala and Atamanczuk, 1998). Soil electrical properties and the applied frequency determine the rate of heat generation (Acierno et al., 2003; Kawala and Atamanczuk, 1998). A microwave applicator for MISD has been developed by Acierno et al. (2004) in a recent pilot study; however, this study is the only field scale study done to date.

2.1.3 Electrical Resistance

Similar to RFH, electrical resistance heating (ERH) applies heat directly to a contaminated zone within regions of low permeability. During ERH, an electrical current is passed through soil resulting in the generation of heat from the energy dissipated due to the resistance provided by the porous media. A schematic of a typical ERH system is shown in Figure 2-3.

As temperatures rise in the subsurface contaminants are vaporized and steam is generated. ERH, like RFH, is limited by soil moisture content. The soil nearest an electrode dries much faster than the bulk soil which leads to increased resistance to energy flow and decreased removal efficiency (EPA, 1997). However, this decrease in efficiency can be overcome with the addition of an aqueous solution containing an

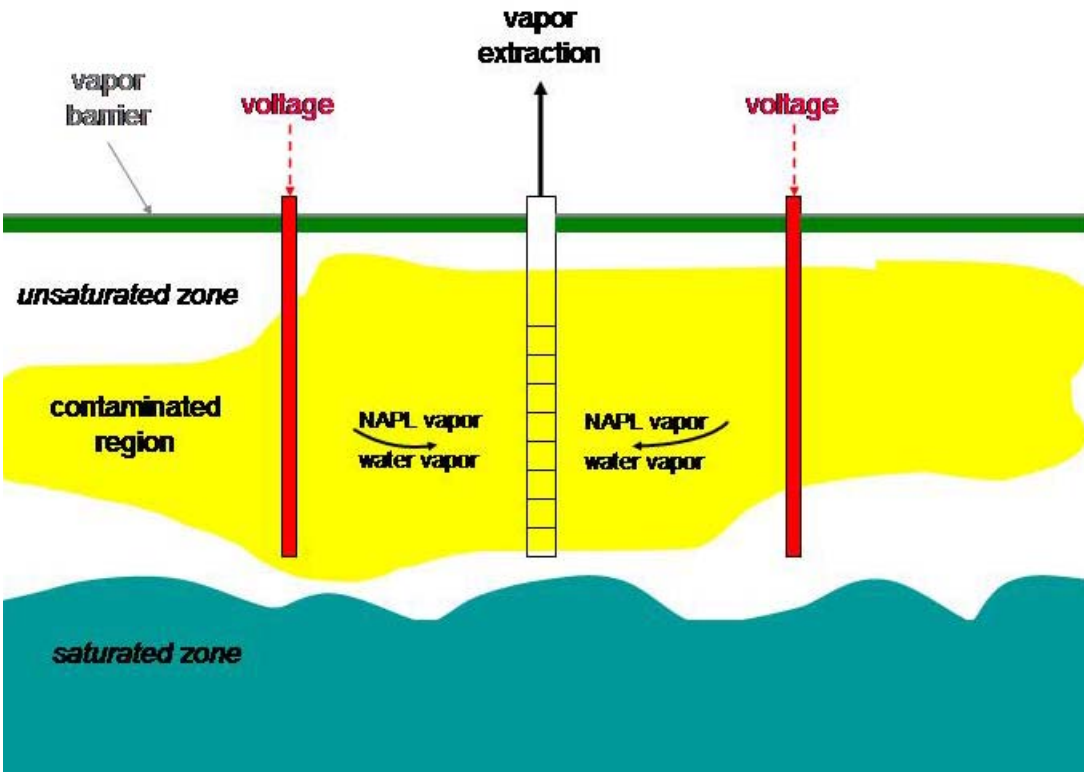

Figure 2-3: Electrical Resistance Heating System Schematic

electrolyte (EPA, 2004; EPA, 1997). Soil characteristics determine the rate of water and electrolyte application required to maintain adequate moisture content. ERH is capable of heating the soil up to 100°C; however, there is some evidence that temperatures up to 200°C may be possible (Dablow III et al., 2000).

Energy is supplied to the system directly from a power line in the form of three-phase electricity. Six-phase power may also be used by splitting three-phase electricity. Six-phase systems exhibit a more uniform heating distribution than three-phase systems; however, the costs associated with converting six-phase electricity may not be worth the increase in uniformity (Buettner and Daily, 1995). For six-phase heating, a trailer-mounted power plant containing a transformer is needed to covert three-phase powerline

frequency energy (EPA, 1997). The transformer also allows energy input to be controlled as the resistance changes due to decreasing water content. Six-phase heating is typically used in pilot scale applications, while three-phase electricity is preferred for full scale operations (Beyke and Fleming, 2005). For either system, each phase is delivered to a single electrode. Electrical phases are shifted to avoid "cold spots" between adjacent electrodes (Buettner and Daily, 1995). In total, six electrodes are used, arranged in a hexagonal pattern with a single SVE well in the center as shown the ERH system schematic, Figure 2-4, below.

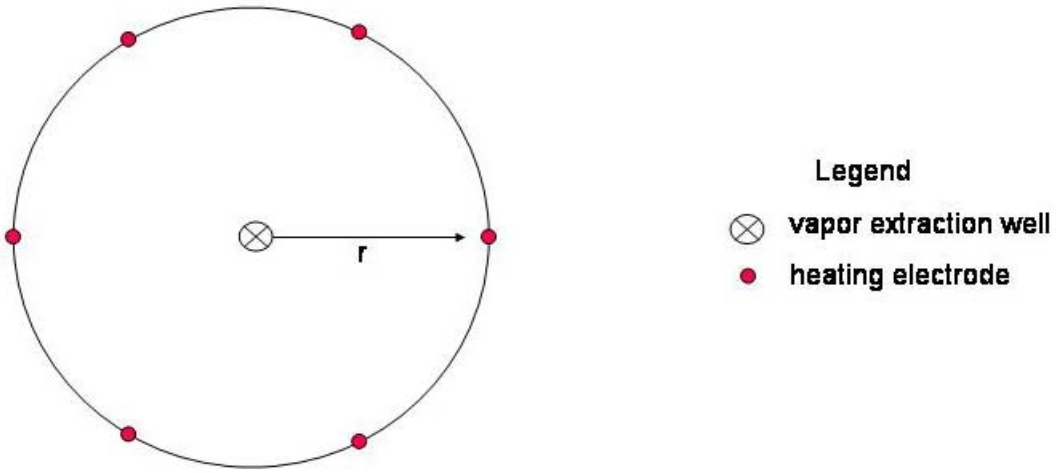

Figure 2-4: Electrical Resistance Heating Electrode Layout

Typical spacing between electrodes ranges from 14 to 24 feet (Beyke and Fleming, 2005). Treatment by ERH usually consists of several overlapping heating arrays with diameters of 30 to 40 feet; however, single arrays of up to 100 feet in diameter can be used (EPA, 2004; Beyke, 1998). The electrical conductivity of the soil

limits the radius of the array (Heine and Steckler, 1999). Voltages can range between 200 and 1,600 volts depending on soil moisture content (EPA, 1997).

2.1.4 Summary and Conclusions

2.1.4.1 Generalized Costs

According to the Remediation Technologies Screening Matrix and Reference Guide, the cost for a thermally enhanced SVE system is approximately $30 to $130 per m^3 of soil treated (Van Deuren et al., 2002). Additional cost data available varies widely for each technology. Recent work done by Beyke and Flemming indicates that a 99% reduction of TCE in soil and groundwater using ERH will cost $200,000 plus an additional $50 to $100 per m^3 Steam injection is estimated to be in the range of $30 to $60 per m^3. Cost information available for RFH suggests that it is in the upper end of the range reported by Van Deuren et al. (2002). Other sources suggest the cost is somewhat higher. Daniel et al. studied two cases where the unit cost was $182 and $288 per m^3 (1999). The figures reported by Daniel et al. account for a number of parameters that may not be included in other sources.

2.1.4.2 Recommendations and Decisionmaking

<u>Steam Injection</u>

Thermally enhanced soil vapor extraction using steam injection is a well established technology. However, site geology is a significant limiting factor. Steam injection is only applicable to sites with moderate to high permeability. Additionally, a

region of low permeability must be present below the zone of contamination to prevent contaminant migration. For shallow applications, a low permeability layer near the surface may be required to prevent steam breakthrough. Soil temperatures will be near the boiling point of water.

Hot Air Injection

Hot air injection is relatively inexpensive. However, hot air injection is not an efficient process due to the comparatively low heat capacity of air

Radiofrequency Heating

RFH is capable of rapidly heating soil to temperatures ranging from 150°C to 200°C. Heating with radiofrequency is comparatively uniform. RFH is well suited for use in low permeability soils because heat is applied directly to the soil. However, such high temperatures can lead to problems associated with soil desiccation, such as fracturing.

Electrical Resistance Heating

ERH is well suited for use in low permeability soils because heat is applied directly to the soil. Electrodes require little disturbance to the soil. Energy required can be supplied directly from a local utility. ERH can heat soil to around 100ºC. ERH depends on soil moisture content and soil drying may be problematic.

Recommendations

Based on these factors, a flow chart was developed to help decision-makers in determining what thermal enhancement methods are applicable for a particular site.

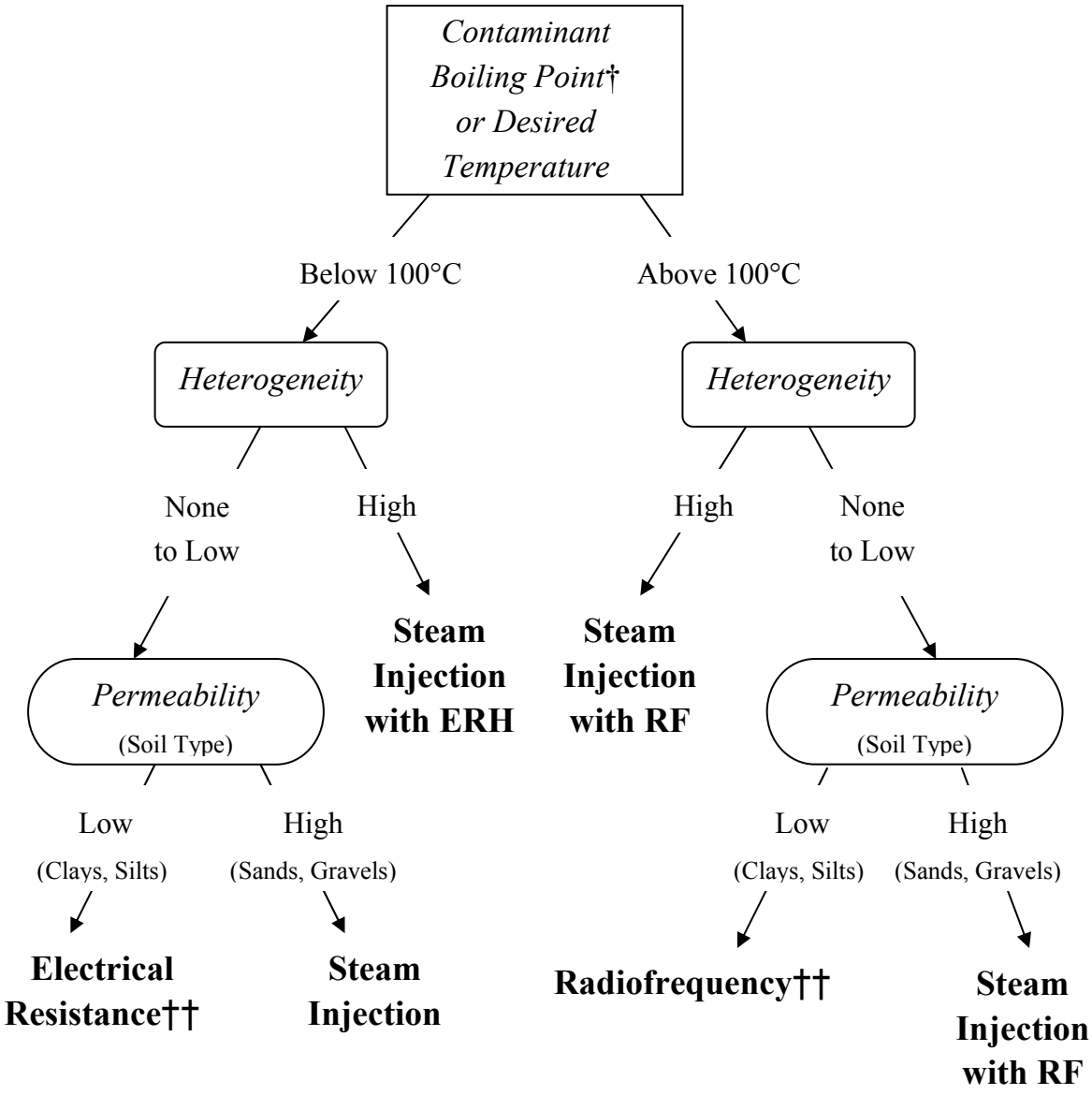

†- choose the highest boiling point of all contaminants

††- water addition may be needed at sites with low moisture content

Figure 2-6: Decision Tool for Selecting Most Appropriate Heating Technique

2.2 Previous Approaches and Modeling

Modeling of heat and mass transfer within a porous media has been studied by numerous authors. Only the most relevant previous work is surveyed here. Numerical modeling of steam injection in shallow applications has been studied at length by Falta et al. (1992). The authors developed STMVOC a three phase (gas, liquid, NAPL) three component system (air, water, NAPL). This simulator allows for each phase to flow. Three mass balance equations, one energy balance equation and a set of primary and secondary variables are used to describe the system. The key assumptions used in the formulation of STMVOC are outlined as follows:

- Local chemical and thermal equilibrium exists between the three phases,
- No chemical reactions are occurring except mass transfer and adsorption,
- Mass transfer in the NAPL phase includes evaporation and boiling,
- Mass transfer by condensation and dissolution are also considered,
- Both the latent and sensible heat are considered to account for phase transitions.

The governing balance equations are generally written for a flow region, V_l, with a surface area Γ_l:

$$\frac{\partial}{\partial t}\int_{V_l} M^K \, dV_l = \int_{\Gamma_l} F^K \cdot n \, d\Gamma_l + \int_{V_l} q^K \, dV_l \qquad 2\text{-}1$$

The method of Abriola and Pinder (1985) was used to prevent complete disappearance or appearance of a phase due to the complexity of the appearance/disappearance mechanisms. This method uses a minimum saturation value for the NAPL phase of 10^{-4}. The minimum saturation is used in combination with "pseudo" gas phase NAPL concentration which limits evaporation.

$$\hat{C}_g^c \approx \left(\frac{S_n}{S_n + 10^{-4}} \right) \overline{C}_g^c \qquad 2\text{-}2$$

Incorporating Henry's constant with equation 2-2 prevents complete disappearance of the NAPL phase. The authors believe the simplicity of this method overrides the inability to completely characterize NAPL removal. Finally, STMVOC is solved using MULKOM (Press, 1983; 1987). MULKOM is a general integral finite difference solver designed for multiphase heat and mass transport.

Adenekan et al. (1993) developed M^2NOTS, a numerical simulator for multicomponent multiphase transport of contaminants and heat from an injection source. Unlike the previous work by Falta et al. (1992), the model presented allows for the complete appearance/disappearance of each phase and any component can partition into any fluid phase present. This simulator also accounts for three flowing phases (air, water, NAPL), like the previous work by Falta et al. (1992). The primary assumptions made are:

- Local chemical and thermal equilibrium,
- Multiphase fluid flow is sufficiently described by the Darcy equation,
- Gravitational and viscous forces are neglected in the energy balance,
- Adsorption follows a linear isotherm,
- No chemical reactions are occurring.

The set of governing equations presented are conservation of mass for each component, energy balance and Darcy's Law. The conservation of mass is:

$$\frac{\partial}{\partial t}\left[(1-\varphi)\frac{\rho_r' w_{ir}}{M_i} + \varphi \sum_{\beta=w,o,g} S_\beta \rho_\beta x_{i\beta} \right] = -\nabla \cdot \mathbf{F}_i + q_i \qquad 2\text{-}3$$

The energy balance is:

$$\frac{\partial}{\partial t}\left[(1-\varphi)\rho_r' C_{p_r} T + \varphi \sum_{\beta=w,o,g} S_\beta \rho_\beta' U_\beta\right] = -\nabla \cdot \left[\sum_{\beta=w,o,g} H_\beta \rho_\beta \frac{\kappa k_{r\beta}}{\mu_\beta} \cdot \left(\nabla P_\beta - \rho_\beta' \mathbf{g}\right) + \boldsymbol{\lambda} \cdot \nabla T\right] + q_{heat} \quad \text{2-4}$$

Darcy's law is written as:

$$\mathbf{F}_i = -\left[\sum_{\beta=w,o,g} \rho_\beta x_{i\beta} \frac{\kappa k_{r\beta}}{\mu_\beta} \cdot \left(\nabla P_\beta - \rho_\beta' \mathbf{g}\right) + \varphi S_\beta \tau_\beta \rho_\beta \mathrm{D}_{i\beta} \cdot \nabla x_{i\beta}\right] \quad \text{2-5}$$

The integral finite difference method is used to solve the system of equations by discretizing the flow domain into arbitrarily shaped polyhedrons.

A proof of concept demonstration of electrical heating completed in the summer of 1992 was modeled by Buettner and Daily (1995). The simplistic model is based on a generic heat equation with a heat source term.

$$\frac{\partial T}{\partial t} = \left(\frac{k}{C\rho}\right)\nabla^2 T + \frac{U}{C\rho} \quad \text{2-6}$$

The source term is based on the electrical conductivity of the soil and the electric field applied. This simplistic method allows the initial heating rates to be studied. The authors make the argument that at early time the temperature will vary linearly with time. Calculations are carried out for a three-phase system and a six-phase electrical system. The results show that the heating-rate distribution during the first 10 days shows, as discussed in Section 2.1.3, six-phase heating is somewhat more uniform than heating with three-phase power.

Electrical heating has been studied on a laboratory scale by Heron et al. (1998). In this study, the effect of heating soil to near the boiling point of TCE (85°C) and water

(100°C) to enhance remediation was demonstrated. Soil temperature reached 85°C after 13 days of heating and 100°C after 34 days of heating. Striking reductions in concentration were seen after reaching 85°C. At 100°C, steam was produced due to the boiling of water and TCE flux reached a maximum as the soil temperature was maintained above 99°C. Heron et al. (1998) reported that TCE flux remained high even when the residual concentration was low. This observation indicated that tailing may be less significant using thermally enhanced SVE rather than traditional SVE. Results suggested that sorption is still an important mechanism, though the importance may be somewhat reduced than with a traditional SVE system.

Electrical heating has been studied at the laboratory scale by Carrigan and Nitao (2000). The basic ohmic heating model employs a conservation of electric charge equation and Ohm's law. The numerical solution of the heating model employs the superposition of two single-phase solutions. Superposition is necessary because of the time dependent nature of the authors set of equations. The model was used to show the temperature distribution and uniformity of an electrical heating system. As indicated by Buettner and Daily (1995), a six-phase system is shown to be the most uniform. Since vapors condense outside of the heated region, the authors suggest that electrical heating should be used in conjunction with steam injection to target liquid-phase contaminants in areas of high permeability.

Benard et al. have studied boiling in porous media (2005). The model developed for heat and mass transfer in porous media uses a set of governing equations consisting of mass conservation and two energy equations based on the first and second law of thermodynamics, Figures 2-7 and 2-8 respectively.

$$\frac{\partial E}{\partial t} = -\nabla \cdot \sum_{p=l,v} h_{\mathrm{P}} \rho_{\mathrm{P}} \mathbf{v}_{\mathrm{P}} - \nabla \cdot \mathbf{q} + \mathbf{g} \cdot \sum_{p=l,v} \rho_{\mathrm{P}} \mathbf{v}_{\mathrm{P}} + \bar{Q} \qquad 2\text{-}7$$

$$\frac{\partial \tilde{\eta}}{\partial t} \geq -\nabla \cdot \left(\sum_{p=l,v} \eta_{\mathrm{P}} \rho_{\mathrm{P}} \mathbf{v}_{\mathrm{P}} + \frac{\mathbf{q}}{T} \right) + \frac{\bar{Q}}{T} \qquad 2\text{-}8$$

The authors propose that three equilibrium states are possible based on the Gibbs potential: 1) liquid-vapor equilibrium 2) no liquid phase present and 3) no vapor phase present. These conditions along with others allow the thermodynamic state to be assessed any point in the system. Phase transitions are managed by using a finite volume method, specifically Newton's method. This method allows the thermodynamic state to be updated with each iteration; therefore, no minimum saturation value is required. Additionally, the method does not require the assumption of that the liquid and vapor phases be present everywhere.

In the model proposed by Benard et al. (2005), evaporation and condensation are accounted for in the mass balance by setting the continuity equation equal to the mass rate of water transferred from the vapor phase to the liquid phase in the case of condensation and equal to the mass rate of water transferred from the liquid phase to the vapor phase in the case of evaporation. This methodology was employed in the model presented in Chapter 3 of this work.

CHAPTER III

MODEL DEVELOPMENT

3.1 Conceptual Model

The symmetry of the electrical resistance heating system, shown in Figure 3-1, allowed for the use of a representative slice – $1/6^{th}$ of the circular heating array – as a basis for examination of air flow and heat transfer within the array. The representative slice is shown below in Figure 3-1.

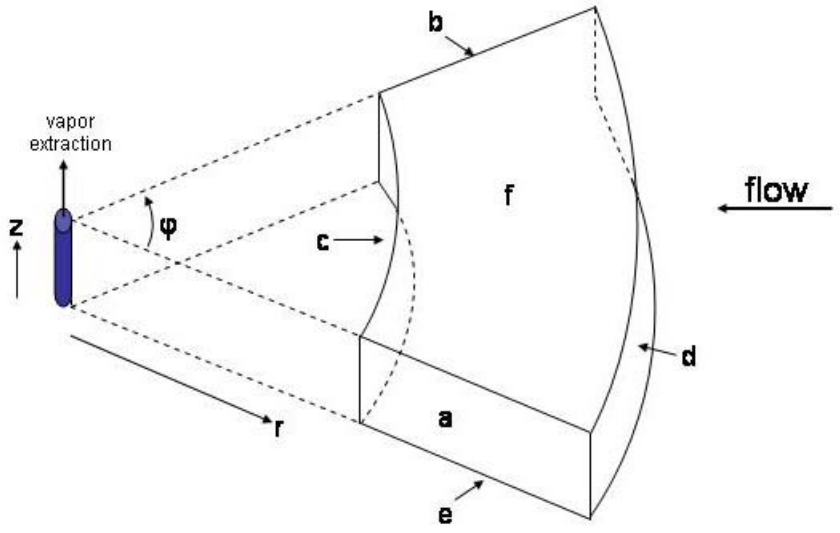

Figure 3-1: Representative Slice

Any surface from the figure above can be visualized as a section of the porous medium, which consists of soil particles, contaminants, water and air as represented in Figure 3-2. It is important to note that only the air phase is continuous and the solid is inert.

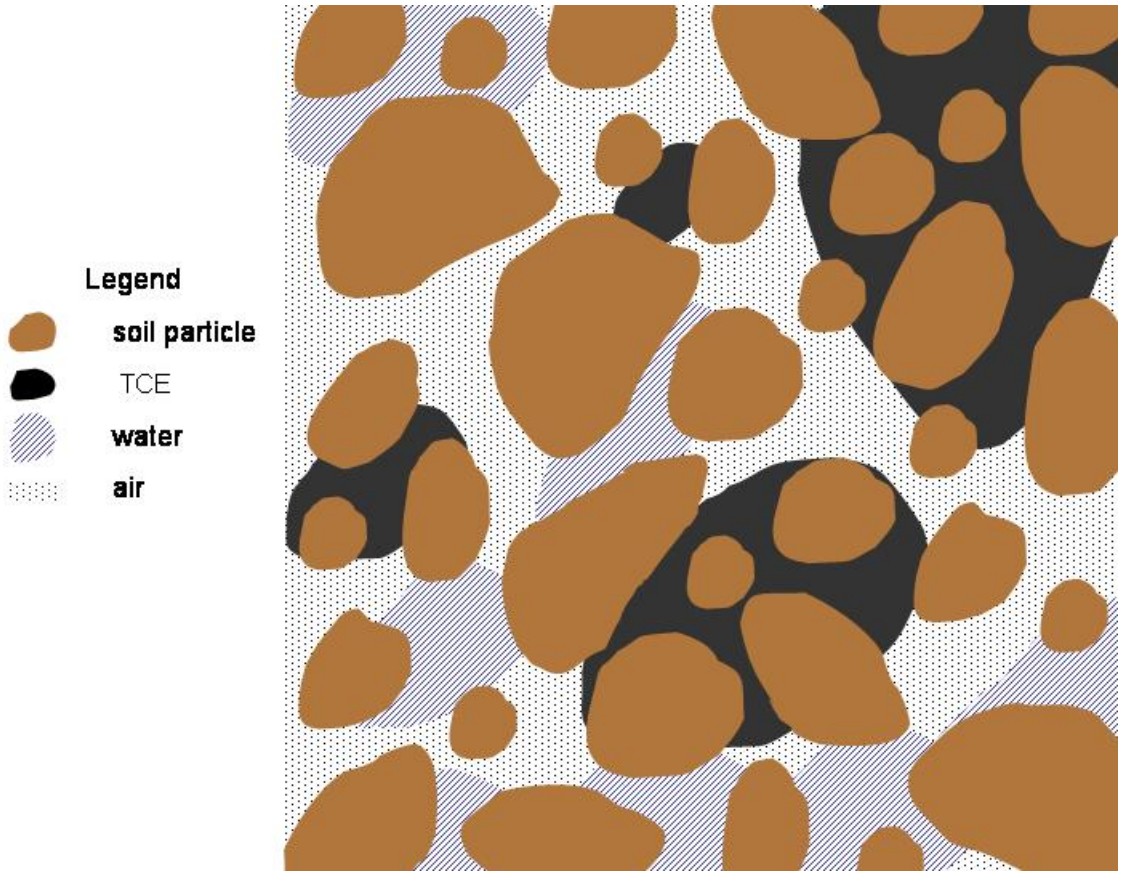

Figure 3-2: Porous Medium Control Volume

The area and volume within the porous medium available for gas and liquid flow across each surface (a thru f) in the diagram is listed in Table 3-1. The table is used extensively in the following section in the derivations of the governing equations for conservation of mass, momentum and energy.

Table 3-1: Flow Areas and Volumes

Directional Coordinate	Surface	Cross-sectional Areas for System with 4 Physical Phases		Total Area
		Gas Flow	Liquid Flow	
r	c	$\eta\theta_{g,c}r\Delta\varphi\Delta z$	$\eta\theta_{l,c}r\Delta\varphi\Delta z$	$r\Delta\varphi\Delta z$
r	d	$\eta\theta_{g,c}(r+\Delta r)\Delta\varphi\Delta z$	$\eta\theta_{l,c}(r+\Delta r)\Delta\varphi\Delta z$	$(r+\Delta r)\Delta\varphi\Delta z$
φ	a	$\eta\theta_{g,c}\Delta r\Delta z$	$\eta\theta_{l,c}\Delta r\Delta z$	$\Delta r\Delta z$
φ	b	$\eta\theta_{g,c}\Delta r\Delta z$	$\eta\theta_{l,c}\Delta r\Delta z$	$\Delta r\Delta z$
z	e	$\eta\theta_{g,c}r\Delta r\Delta\varphi$	$\eta\theta_{l,c}r\Delta r\Delta\varphi$	$r\Delta r\Delta\varphi$
z	f	$\eta\theta_{g,c}r\Delta r\Delta\varphi$	$\eta\theta_{l,c}r\Delta r\Delta\varphi$	$r\Delta r\Delta\varphi$
Volume		$\eta\theta_{g,c}r\Delta r\Delta\varphi\Delta z$	$\eta\theta_{l,c}r\Delta r\Delta\varphi\Delta z$	$r\Delta r\Delta\varphi\Delta z$

The porous medium is conceptually represented by four separate phases – soil particle (solid), liquid water, liquid TCE (NAPL), and gas – with interactions due to advection, sorption, dissolution, evaporation-condensation and convection-conduction processes. The dominant mechanisms considered here are evaporation and condensation (NAPL, water and air components) and heat transfer by conduction and convection (all components) illustrated in Figure 3-3. Air flow is typically saturated with respect to water and NAPL (TCE) at a reference temperature and pressure.

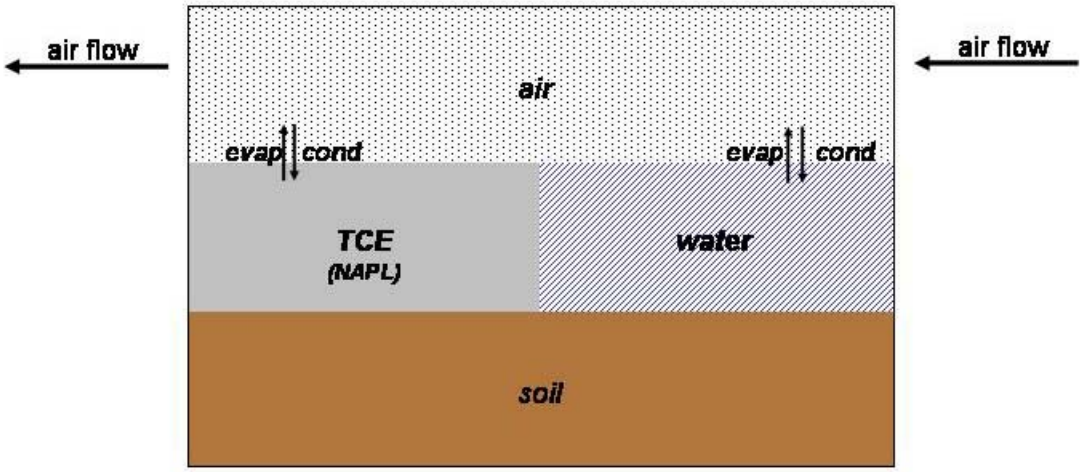

Figure 3-3: Conceptual Representation of the Phases and Their Interactions

Water and contaminants are vaporized as the temperature near the electrode reaches the boiling point. The vapors are then pushed toward the extraction well (r_w) by the flowing air phase as illustrated in Figure 3-4.

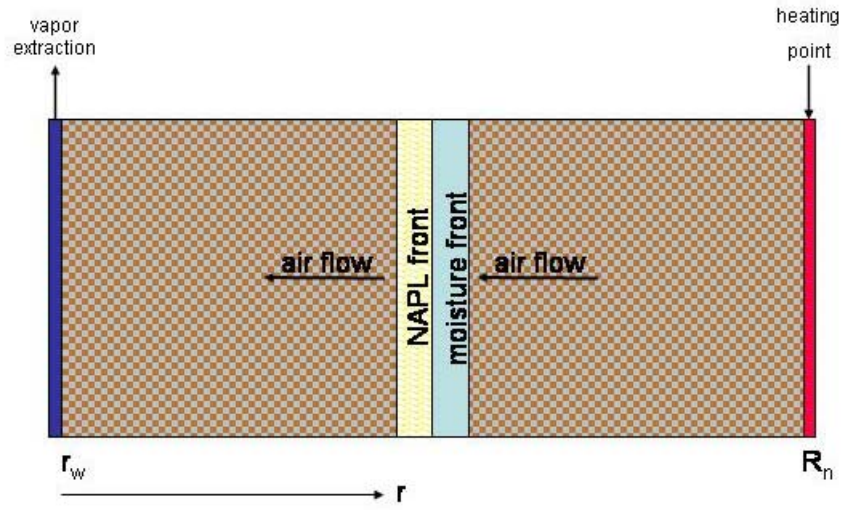

Figure 3-4: Radial Flow within the Porous Medium

When the vapors reach cooler regions the NAPL and water will condense and then be reheated as the temperature profile extends toward the vapor extraction well. This process occurs repeatedly until the entire circular area is heated thoroughly and vapors are removed at the vapor extraction well. Figure 3-5 demonstrates the temperature profile expected throughout the region.

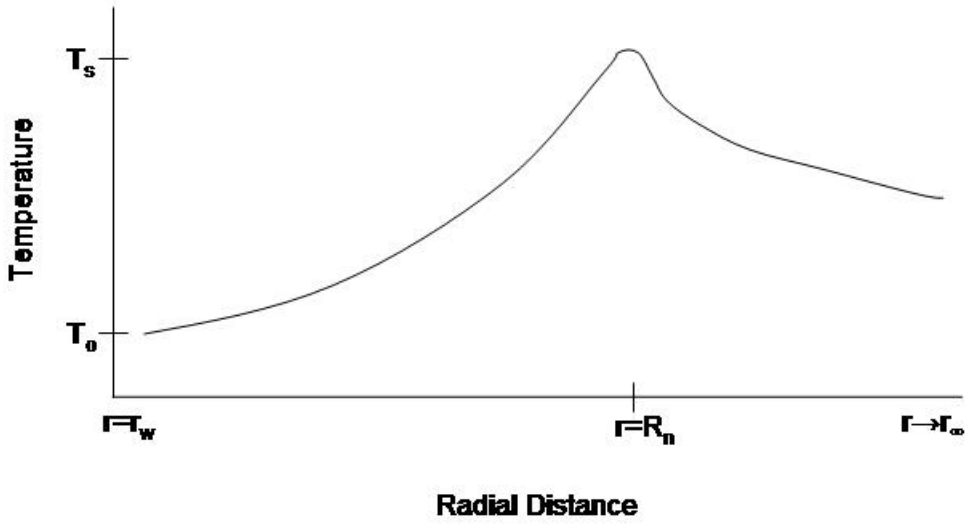

Figure 3-5: Temperature Profile

This process results in a "hot" area of low water content behind the condensation front (Figure 3-6).

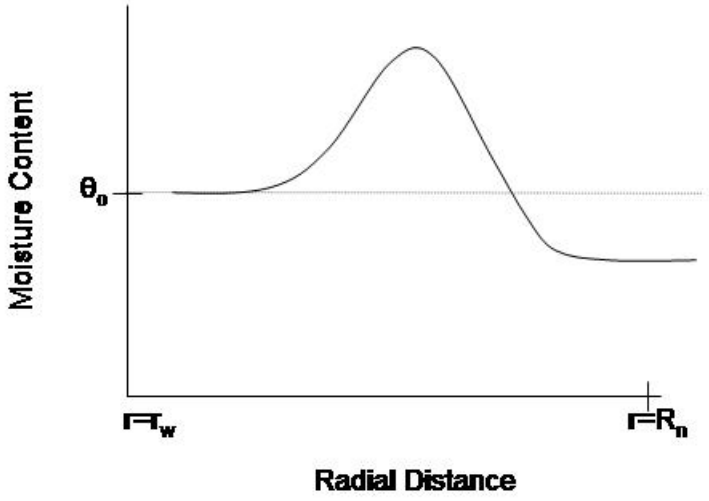

Figure 3-6: Moisture Content along the Radial Axis

The pressure distribution, illustrated in Figure 3-7, increases with radial distance.

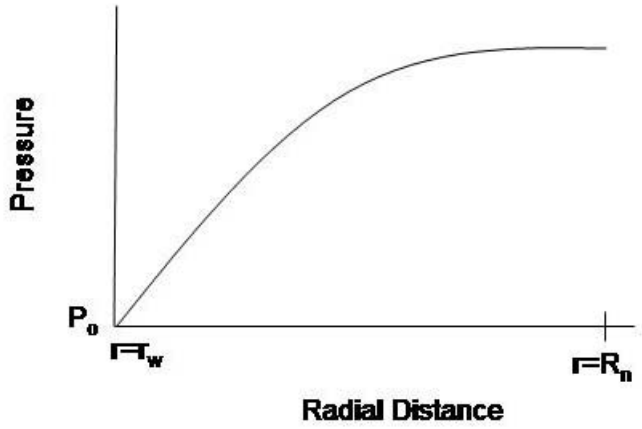

Figure 3-7: Pressure Profile

3.2 Governing Equations

Governing equations for the conservation of mass, momentum and energy are derived for the most general case following the shell balance approach of Bird, Stewart and Lightfoot (1960). Then, the general equations are written for a multiphase multicomponent system according to Table 3-2, which illustrates possible phase-component combinations.

Table 3-2: Phase-Component Possibilities

	Phase (β)		
	Liquid	*Gas*	*Solid*
Component (α)			
soil			X
air		X	
TCE	X (NAPL)	X	
water	X	X	

X denotes phase-component combination

The following assumptions were made in the derivation of each conservation equation. The gas phase is compressible and the ideal gas law applies. The liquid phase is incompressible and immobile. The solid is considered to be inert – sorption is not considered. The air phase is composed primarily of nitrogen; therefore, physical properties of air will be based on N_2. The thickness of the porous medium is constant. The porosity is constant. Several additional assumptions were made for the conservation of energy equation. The system is nonisothermal, nonadiabatic, nonisentropic. Local thermal equilibrium (i.e., $T_s=T_{NAPL}=T_{air}=T_{water}$) is assumed (Falta et al., 1992; Adenekan et al., 1993; Benard et al., 2005). Viscous forces are negligible in comparison to the heat transfer process (Adenekan et al., 1993). Internal energy is much larger than kinetic energy; therefore, kinetic energy is neglected. Potential energy is assumed negligible as well (Adenekan et al., 1993).

3.2.1 Conservation of Mass

The governing conservation of mass equation is derived from applying the Reynolds Transport Theorem over a differential control volume:

$$\frac{\partial}{\partial t}\iiint_{CV} \eta\theta\rho \, dV + \iint_{CS} \rho(v \cdot n) \, dA = \dot{m}V \tag{3.1}$$

Integrations are performed over the entire differential control volume and control surface as shown in Figures 3.3 and 3.1, respectively.

$$\frac{\partial}{\partial t}\eta\theta\rho V + \rho(-\mathbf{v}_a A_a + \mathbf{v}_b A_b - \mathbf{v}_c A_c + \mathbf{v}_d A_d - \mathbf{v}_e A_e + \mathbf{v}_f A_f) = \dot{m}V \tag{3.2}$$

Volume, area and velocity components from Table 3.1 are substituted into the above equation

$$\begin{aligned}\frac{\partial}{\partial t}\eta\theta\rho(\eta\theta r\Delta r\Delta\varphi\Delta z) &+ \eta\theta\Delta r\Delta z\left[\left(\rho+\frac{\partial\rho}{\partial t}\right)\left(\mathbf{v}_\varphi+\frac{\partial\mathbf{v}_\varphi}{\partial t}\right)-\rho\mathbf{v}_\varphi\right] \\ &+\eta\theta\Delta\varphi\Delta z\left[\left(r+\Delta r\right)\left(\rho+\frac{\partial\rho}{\partial t}\right)\left(\mathbf{v}_r+\frac{\partial\mathbf{v}_r}{\partial t}\right)-r\rho\mathbf{v}_r\right] \\ &+\eta\theta r\Delta r\Delta z\left[\left(\rho+\frac{\partial\rho}{\partial t}\right)\left(\mathbf{v}_z+\frac{\partial\mathbf{v}_z}{\partial t}\right)-\rho\mathbf{v}_z\right] = \dot{m}(\eta\theta r\Delta r\Delta\varphi\Delta z)\end{aligned} \tag{3.3}$$

The relationship is divided by volume $(\eta\theta r\Delta r\Delta\varphi\Delta z)$ and the limit as Δr, $\Delta\varphi$, and Δz approach zero is taken to obtain

$$\frac{\partial}{\partial t}\eta\theta\rho + \frac{1}{r}\frac{\partial}{\partial r}(r\rho\mathbf{v}_r) + \frac{1}{r}\frac{\partial}{\partial\varphi}(\rho\mathbf{v}_\varphi) + \frac{\partial}{\partial z}(\rho\mathbf{v}_z) = \dot{m} \tag{3.4}$$

which can be rewritten as the equation of continuity

$$\frac{\partial}{\partial t}\eta\theta\rho + (\nabla \cdot \rho\mathbf{v}) = \dot{m} \tag{3.5}$$

The rate of mass transferred per unit volume per time ($\dot{m}$) is

$$\dot{m} = \pm \frac{\mathbf{q}}{\mathrm{h}_{\mathrm{vap}}} \tag{3.6}$$

where (+) indicates evaporation and (-) indicates condensation. For a multicomponent multiphase system the governing equation for conservation of mass is:

$$\frac{\partial}{\partial t} \eta \theta_{\alpha,\beta} \rho_{\alpha,\beta} + (\nabla \cdot \mathbf{v}_{\alpha,\beta}) = \pm \frac{\mathbf{q}}{\mathrm{h}_{\mathrm{vap}}} \tag{3.7}$$

For the components TCE, air, and water, the equation for conservation of mass in the gas phase is:

$$\frac{\partial}{\partial t} \eta \theta_{g;TCE,\,N_2,water} \rho_{g;TCE,\,N_2,water} + (\nabla \cdot \rho_{g;TCE,\,N_2,water} \mathbf{v}_{g;TCE,\,N_2,water}) = \pm \frac{\mathbf{q}}{\mathrm{h}_{\mathrm{vap}}} \tag{3.8}$$

Since the liquid phase is immobile in this system ($\mathbf{v}_l = 0$), conservation of mass is written as:

$$\frac{\partial}{\partial t} \eta \theta_{l;TCE,\,N_2,water} \rho_{l;TCE,\,N_2,water} = \pm \frac{\mathbf{q}}{\mathrm{h}_{\mathrm{vap}}} \tag{3.9}$$

3.2.2 Conservation of Momentum

Similarly, the governing equation for conservation of mass is derived from the Reynolds Transport Theorem applied to the differential control volume shown in Figure 3.1:

$$\frac{\partial}{\partial t} \iiint_{CV} \mathbf{v} \rho \, \mathrm{dV} + \iint_{CS} \mathbf{v} \rho (\nu \cdot n) \, \mathrm{dA} = \sum \mathrm{F} \tag{3.10}$$

Integrating over the differential control volume and control surface for the gas phase as shown in Figures 3.3 and 3.1, respectively:

$$\frac{\partial}{\partial t}\left(\mathbf{v}\rho\ dV\right)+\mathbf{v}\rho\left(-\mathbf{v}_a A_a+\mathbf{v}_b A_b-\mathbf{v}_c A_c+\mathbf{v}_d A_d-\mathbf{v}_e A_e+\mathbf{v}_f A_f\right)=F_g - F_P - F_v \qquad (3.11)$$

Volume, area and velocity components from Table 3.1 can be substituted into the above equation

$$\begin{aligned}\frac{\partial}{\partial t}\left(\mathbf{v}\rho\eta\theta r\Delta r\Delta\varphi\Delta z\right)&+\mathbf{v}\rho\Delta r\Delta z\eta\theta\left[\left(\mathbf{v}_\varphi+\frac{\partial\mathbf{v}_\varphi}{\partial\varphi}\right)-\mathbf{v}_\varphi\right]\\&+\mathbf{v}\rho\Delta\varphi\Delta z\eta\theta\left[\left(r+\Delta r\right)\left(\mathbf{v}_r+\frac{\partial\mathbf{v}_r}{\partial r}\right)-r\mathbf{v}_r\right]\\&+\mathbf{v}\rho r\Delta r\Delta\varphi\eta\theta\left[\left(\mathbf{v}_z+\frac{\partial\mathbf{v}_z}{\partial z}\right)-\mathbf{v}_z\right]=F_g+F_P+F_v\end{aligned} \qquad (3.12)$$

The relationships for the forces are

$$F_g=\iiint_{CV}\rho\mathbf{g}\ dV \qquad \text{(gravity)} \qquad (3.13)$$

$$F_P=\iint_{CS}P\ dA \qquad \text{(pressure)} \qquad (3.14)$$

$$F_v=\iint_{CS}\left(\boldsymbol{\tau}\cdot n\right)dA \qquad \text{(viscous)} \qquad (3.15)$$

Performing the integrations in (3.13), (3.14), and (3.15)

$$F_g=\rho\mathbf{g}r\Delta r\Delta\varphi\Delta z \qquad (3.16)$$

$$F_P=-P_aA_a+P_bA_b-P_cA_c+P_dA_d-P_eA_e+P_fA_f \qquad (3.17)$$

$$F_v=-\boldsymbol{\tau}_aA_a+\boldsymbol{\tau}_bA_b-\boldsymbol{\tau}_cA_c+\boldsymbol{\tau}_dA_d-\boldsymbol{\tau}_eA_e+\boldsymbol{\tau}_fA_f \qquad (3.18)$$

Pressure and area over the control surface can be substituted into (3.17).

$$F_P = \Delta r\Delta z\left[\left(P_\varphi + \frac{\partial P_\varphi}{\partial \varphi}\right) - P_\varphi\right] + \Delta\varphi\Delta z\left[\left(r+\Delta r\right)\left(P_r + \frac{\partial P_r}{\partial r}\right) - rP_r\right] + r\Delta r\Delta\varphi\left[\left(P_z + \frac{\partial P_z}{\partial z}\right) - P_z\right] \tag{3.19}$$

Viscous forces and area for the control surface can be substituted into (3.18).

$$\begin{aligned} F_v = {} & \Delta\varphi\Delta z\left\{\left[\left(r+\Delta r\right)\left(\boldsymbol{\tau}_{rr} + \frac{\partial \boldsymbol{\tau}_{rr}}{\partial r}\right) - r\boldsymbol{\tau}_{rr}\right] + \left[\left(r+\Delta r\right)\left(\boldsymbol{\tau}_{r\varphi} + \frac{\partial \boldsymbol{\tau}_{r\varphi}}{\partial r}\right) - r\boldsymbol{\tau}_{r\varphi}\right] + \left[\left(r+\Delta r\right)\left(\boldsymbol{\tau}_{rz} + \frac{\partial \boldsymbol{\tau}_{rz}}{\partial r}\right) - r\tau_{rz}\right]\right\} \\ & + \Delta r\Delta z\left\{\left[\left(\boldsymbol{\tau}_{\varphi r} + \frac{\partial \boldsymbol{\tau}_{\varphi r}}{\partial \varphi}\right) - \boldsymbol{\tau}_{\varphi r}\right] + \left[\left(\boldsymbol{\tau}_{\varphi\varphi} + \frac{\partial \boldsymbol{\tau}_{\varphi\varphi}}{\partial \varphi}\right) - \boldsymbol{\tau}_{\varphi\varphi}\right] + \left[\left(\boldsymbol{\tau}_{\varphi z} + \frac{\partial \boldsymbol{\tau}_{\varphi z}}{\partial \varphi}\right) - \boldsymbol{\tau}_{\varphi z}\right]\right\} \\ & + r\Delta r\Delta\varphi\left\{\left[\left(\boldsymbol{\tau}_{zr} + \frac{\partial \boldsymbol{\tau}_{zr}}{\partial \varphi}\right) - \boldsymbol{\tau}_{zr}\right] + \left[\left(\boldsymbol{\tau}_{z\varphi} + \frac{\partial \boldsymbol{\tau}_{z\varphi}}{\partial z}\right) - \boldsymbol{\tau}_{z\varphi}\right] + \left[\left(\boldsymbol{\tau}_{zz} + \frac{\partial \tau_{zz}}{\partial \varphi}\right) - \boldsymbol{\tau}_{zz}\right]\right\} \end{aligned} \tag{3.20}$$

The relationships for gravitational, pressure and viscous forces [(3.16), (3.19) and (3.20)] are substituted into right hand side of equation (3.12).

$$
\begin{aligned}
&\frac{\partial}{\partial t}\left(\mathbf{v}\rho\eta\theta r\Delta r\Delta\varphi\Delta z\right)+\mathbf{v}\rho\left\{\Delta r\Delta z\eta\theta\left[\left(\mathbf{v}_{\varphi}+\frac{\partial\mathbf{v}_{\varphi}}{\partial\varphi}\right)-\mathbf{v}_{\varphi}\right]\right.\\
&\left.+\Delta\varphi\Delta z\eta\theta\left[\left(r+\Delta r\right)\left(\mathbf{v}_{r}+\frac{\partial\mathbf{v}_{r}}{\partial r}\right)-r\mathbf{v}_{r}\right]+r\Delta r\Delta\varphi\eta\theta\left[\left(\mathbf{v}_{z}+\frac{\partial\mathbf{v}_{z}}{\partial z}\right)-\mathbf{v}_{z}\right]\right\}\\
&=\rho\mathbf{g}r\Delta r\Delta\varphi\Delta z-\Delta r\Delta z\left[\left(P_{\varphi}+\frac{\partial P_{\varphi}}{\partial\varphi}\right)-P_{\varphi}\right]\\
&+\Delta\varphi\Delta z\left[\left(r+\Delta r\right)\left(P_{r}^{\varepsilon}+\frac{\partial P_{r}}{\partial r}\right)-rP_{r}\right]+r\Delta r\Delta\phi\left[\left(P_{z}+\frac{\partial P_{z}}{\partial z}\right)-P_{z}\right]\\
&-\Delta\varphi\Delta z\left\{\left[\left(r+\Delta r\right)\left(\boldsymbol{\tau}_{rr}+\frac{\partial\boldsymbol{\tau}_{rr}}{\partial r}\right)-r\boldsymbol{\tau}_{rr}\right]+\left[\left(r+\Delta r\right)\left(\boldsymbol{\tau}_{r\varphi}+\frac{\partial\boldsymbol{\tau}_{r\varphi}}{\partial r}\right)-r\boldsymbol{\tau}_{r\varphi}\right]\right.\\
&\left.+\left[\left(r+\Delta r\right)\left(\boldsymbol{\tau}_{rz}+\frac{\partial\boldsymbol{\tau}_{rz}}{\partial r}\right)-r\tau_{rz}\right]\right\}+\Delta r\Delta z\left\{\left[\left(\boldsymbol{\tau}_{\varphi r}+\frac{\partial\boldsymbol{\tau}_{\varphi r}}{\partial\varphi}\right)-\boldsymbol{\tau}_{\varphi r}\right]\right.\\
&\left.+\left[\left(\boldsymbol{\tau}_{\varphi\varphi}+\frac{\partial\boldsymbol{\tau}_{\varphi\varphi}}{\partial\varphi}\right)-\boldsymbol{\tau}_{\varphi\varphi}\right]+\left[\left(\boldsymbol{\tau}_{\varphi z}+\frac{\partial\boldsymbol{\tau}_{\varphi z}}{\partial\varphi}\right)-\boldsymbol{\tau}_{\varphi z}\right]\right\}\\
&+r\Delta r\Delta\varphi\left\{\left[\left(\boldsymbol{\tau}_{zr}+\frac{\partial\boldsymbol{\tau}_{zr}}{\partial\varphi}\right)-\boldsymbol{\tau}_{zr}\right]+\left[\left(\boldsymbol{\tau}_{z\varphi}+\frac{\partial\boldsymbol{\tau}_{z\varphi}}{\partial z}\right)-\boldsymbol{\tau}_{z\varphi}\right]+\left[\left(\boldsymbol{\tau}_{zz}+\frac{\partial\tau_{zz}}{\partial\varphi}\right)-\boldsymbol{\tau}_{zz}\right]\right\}
\end{aligned}
\tag{3.21}
$$

Dividing (3.21) by volume $\left(\eta\theta r\Delta r\Delta\varphi\Delta z\right)$ and taking the limit as Δr, $\Delta\varphi$, and Δz approach zero:

$$
\begin{aligned}
&\frac{\partial}{\partial t}\left(\mathbf{v}\rho\right)+\mathbf{v}\left\{\frac{1}{r}\frac{\partial}{\partial r}\left(r\rho\mathbf{v}_{r}\right)+\frac{1}{r}\frac{\partial}{\partial\varphi}\left(\rho\mathbf{v}_{\varphi}\right)+\frac{\partial}{\partial z}\left(\rho\mathbf{v}_{z}\right)\right\}\\
&=\frac{\rho\mathbf{g}}{\eta\theta}-\frac{1}{\eta\theta}\left\{\frac{1}{r}\frac{\partial}{\partial r}\left(rP_{r}\right)+\frac{1}{r}\frac{\partial P_{\varphi}}{\partial\varphi}+\frac{\partial P_{z}}{\partial z}\right\}\\
&-\eta\theta\left\{\frac{1}{r}\frac{\partial}{\partial r}\left(r\boldsymbol{\tau}_{rr}\right)+\frac{1}{r}\frac{\partial}{\partial r}\left(r\boldsymbol{\tau}_{r\varphi}\right)+\frac{1}{r}\frac{\partial}{\partial r}\left(r\boldsymbol{\tau}_{rz}\right)+\frac{1}{r}\frac{\partial}{\partial\varphi}\left(\boldsymbol{\tau}_{\varphi r}\right)\right.\\
&\left.+\frac{1}{r}\frac{\partial}{\partial\varphi}\left(\boldsymbol{\tau}_{\varphi\varphi}\right)+\frac{1}{r}\frac{\partial}{\partial\varphi}\left(\boldsymbol{\tau}_{\varphi z}\right)+\frac{\partial}{\partial z}\left(\boldsymbol{\tau}_{zr}\right)+\frac{\partial}{\partial z}\left(\boldsymbol{\tau}_{z\varphi}\right)+\frac{\partial}{\partial z}\left(\boldsymbol{\tau}_{zz}\right)\right\}
\end{aligned}
\tag{3.22}
$$

For simplicity, (3.22) is separated into r, φ and z components

r-component

$$\begin{aligned}&\frac{\partial}{\partial t}\left(\mathbf{v}_{\mathrm{r}}\,\rho\right)+\mathbf{v}_{\mathrm{r}}\frac{\partial}{\partial \mathrm{r}}\left(\rho\mathbf{v}_{\mathrm{r}}\right)+\frac{\mathbf{v}_{\varphi}}{\mathrm{r}}\frac{\partial}{\partial\varphi}\left(\rho\mathbf{v}_{\mathrm{r}}\right)-\frac{\left(\mathbf{v}_{\varphi}\right)^{2}}{\mathrm{r}}+\mathbf{v}_{\mathrm{z}}\frac{\partial}{\partial \mathrm{z}}\left(\rho\mathbf{v}_{\mathrm{r}}\right)\\&=\frac{\rho g_{\mathrm{r}}}{\eta\theta}-\frac{1}{\eta\theta}\left\{\frac{1}{\mathrm{r}}\frac{\partial}{\partial \mathrm{r}}\left(\mathrm{rP}_{\mathrm{r}}\right)\right\}\\&-\eta\theta\left\{\frac{\partial}{\partial \mathrm{r}}\left(\boldsymbol{\tau}_{\mathrm{rr}}\right)+\frac{1}{\mathrm{r}}\frac{\partial}{\partial \mathrm{r}}\left(\boldsymbol{\tau}_{\mathrm{r}\varphi}\right)+\frac{\partial}{\partial \mathrm{r}}\left(\boldsymbol{\tau}_{\mathrm{rz}}\right)+\frac{\boldsymbol{\tau}_{\mathrm{rr}}}{\mathrm{r}}-\frac{\boldsymbol{\tau}_{\varphi\varphi}}{\mathrm{r}}\right\}\end{aligned}\tag{3.23}$$

φ -component

$$\begin{aligned}&\frac{\partial}{\partial t}\left(\mathbf{v}_{\varphi}\rho\right)+\mathbf{v}_{\mathrm{r}}\frac{\partial}{\partial r}\left(\rho\mathbf{v}_{\varphi}\right)+\frac{\mathbf{v}_{\varphi}}{\mathrm{r}}\frac{\partial}{\partial\varphi}\left(\rho\mathbf{v}_{\varphi}\right)+\frac{\mathbf{v}_{\mathrm{r}}\mathbf{v}_{\varphi}}{\mathrm{r}}+\mathbf{v}_{\mathrm{z}}\frac{\partial}{\partial \mathrm{z}}\left(\rho\mathbf{v}_{\varphi}\right)\\&=\frac{\rho g_{\varphi}}{\eta\theta}-\frac{1}{\eta\theta}\left\{\frac{1}{\mathrm{r}}\frac{\partial \mathrm{P}_{\varphi}}{\partial\varphi}\right\}-\eta\theta\left\{\frac{\partial}{\partial r}\left(\boldsymbol{\tau}_{\mathrm{r}\varphi}\right)+\frac{1}{\mathrm{r}}\frac{\partial}{\partial\varphi}\left(\boldsymbol{\tau}_{\varphi\varphi}\right)+\frac{\partial}{\partial z}\left(\boldsymbol{\tau}_{\mathrm{z}\varphi}\right)+2\frac{\boldsymbol{\tau}_{\mathrm{r}\varphi}}{\mathrm{r}}\right\}\end{aligned}\tag{3.24}$$

z-component

$$\begin{aligned}&\frac{\partial}{\partial t}\left(\mathbf{v}_{\mathrm{z}}\rho\right)+\mathbf{v}_{\mathrm{r}}\frac{\partial}{\partial \mathrm{r}}\left(\rho\mathbf{v}_{\mathrm{z}}\right)+\frac{\mathbf{v}_{\varphi}}{\mathrm{r}}\frac{\partial}{\partial\varphi}\left(\rho\mathbf{v}_{\mathrm{z}}\right)+\mathbf{v}_{\mathrm{z}}\frac{\partial}{\partial \mathrm{z}}\left(\rho\mathbf{v}_{\mathrm{z}}\right)=\frac{\rho g_{\mathrm{z}}}{\eta\theta}-\frac{1}{\eta\theta}\left\{\frac{\partial \mathrm{P}_{\mathrm{z}}}{\partial \mathrm{z}}\right\}\\&-\eta\theta\left\{\frac{\partial}{\partial \mathrm{r}}\left(\boldsymbol{\tau}_{\mathrm{rz}}\right)+\frac{1}{\mathrm{r}}\frac{\partial}{\partial\varphi}\left(\boldsymbol{\tau}_{\varphi\mathrm{z}}\right)+\frac{\partial}{\partial z}\left(\boldsymbol{\tau}_{\mathrm{zz}}\right)+\frac{\boldsymbol{\tau}_{\mathrm{rz}}}{\mathrm{r}}\right\}\end{aligned}\tag{3.25}$$

Equations (3.24) – (3.26) may be rewritten as

r-component

$$\begin{aligned}&\frac{\partial}{\partial t}\left(\mathbf{v}_{\mathrm{r}}\rho\right)+\mathbf{v}_{\mathrm{r}}\frac{\partial}{\partial \mathrm{r}}\left(\rho\mathbf{v}_{\mathrm{r}}\right)+\frac{\mathbf{v}_{\varphi}}{\mathrm{r}}\frac{\partial}{\partial\varphi}\left(\rho\mathbf{v}_{\mathrm{r}}\right)-\frac{\left(\mathbf{v}_{\varphi}\right)^{2}}{\mathrm{r}}+\mathbf{v}_{\mathrm{z}}\frac{\partial}{\partial \mathrm{z}}\left(\rho\mathbf{v}_{\mathrm{r}}\right)\\&=\frac{\rho g_{\mathrm{r}}}{\eta\theta}-\frac{1}{\eta\theta}\left\{\frac{1}{\mathrm{r}}\frac{\partial}{\partial \mathrm{r}}\left(\mathrm{rP}_{\mathrm{r}}\right)\right\}\\&-\eta\theta\left\{\frac{1}{\mathrm{r}}\frac{\partial}{\partial \mathrm{r}}\left(\mathrm{r}\boldsymbol{\tau}_{\mathrm{rr}}\right)+\frac{1}{\mathrm{r}}\frac{\partial}{\partial \mathrm{r}}\left(\boldsymbol{\tau}_{\mathrm{r}\varphi}\right)-\frac{\boldsymbol{\tau}_{\varphi\varphi}}{\mathrm{r}}+\frac{\partial}{\partial \mathrm{r}}\left(\boldsymbol{\tau}_{\mathrm{rz}}\right)\right\}\end{aligned}\tag{3.26}$$

φ -component

$$\begin{aligned}&\frac{\partial}{\partial t}\left(\mathbf{v}_{\varphi}\rho\right)+\mathbf{v}_{\mathrm{r}}\frac{\partial}{\partial \mathrm{r}}\left(\rho\mathbf{v}_{\varphi}\right)+\frac{\mathbf{v}_{\varphi}}{\mathrm{r}}\frac{\partial}{\partial\varphi}\left(\rho\mathbf{v}_{\varphi}\right)+\frac{\mathbf{v}_{\mathrm{r}}\mathbf{v}_{\varphi}}{\mathrm{r}}+\mathbf{v}_{z}\frac{\partial}{\partial \mathrm{z}}\left(\rho\mathbf{v}_{\varphi}\right)\\&=\frac{\rho g_{\varphi}}{\eta\theta}-\frac{1}{\eta\theta}\left\{\frac{1}{\mathrm{r}}\frac{\partial \mathrm{P}_{\varphi}}{\partial\varphi}\right\}\\&-\eta\theta\left\{\frac{1}{\mathrm{r}^{2}}\frac{\partial}{\partial \mathrm{r}}\left(\mathrm{r}^{2}\boldsymbol{\tau}_{\mathrm{r}\varphi}\right)+\frac{1}{\mathrm{r}}\frac{\partial}{\partial\varphi}\left(\boldsymbol{\tau}_{\varphi\varphi}\right)+\frac{\partial}{\partial z}\left(\boldsymbol{\tau}_{z\varphi}\right)\right\}\end{aligned}\tag{3.27}$$

z-component

$$\begin{aligned}&\frac{\partial}{\partial t}\left(\mathbf{v}_{z}\rho\right)+\mathbf{v}_{\mathrm{r}}\frac{\partial}{\partial \mathrm{r}}\left(\rho\mathbf{v}_{z}\right)+\frac{\mathbf{v}_{\varphi}}{\mathrm{r}}\frac{\partial}{\partial\varphi}\left(\rho\mathbf{v}_{z}\right)+\mathbf{v}_{z}\frac{\partial}{\partial \mathrm{z}}\left(\rho\mathbf{v}_{z}\right)\\&=\frac{\rho g_{z}}{\eta\theta}-\frac{1}{\eta\theta}\left\{\frac{\partial \mathrm{P}_{z}}{\partial \mathrm{z}}\right\}\\&-\eta\theta\left\{\frac{1}{\mathrm{r}}\frac{\partial}{\partial \mathrm{r}}\left(\mathrm{r}\boldsymbol{\tau}_{\mathrm{r}z}\right)+\frac{1}{\mathrm{r}}\frac{\partial}{\partial\varphi}\left(\boldsymbol{\tau}_{\varphi z}\right)+\frac{\partial}{\partial \mathrm{z}}\left(\boldsymbol{\tau}_{zz}\right)\right\}\end{aligned}\tag{3.28}$$

The relationships for $\boldsymbol{\tau}$ as listed in (3.29), assuming the vapor phase is a Newtonian fluid are substituted into (3.27), (3.28) and (3.29) as appropriate.

$$\begin{aligned}\boldsymbol{\tau}_{\mathrm{r}\mathrm{r}}&=-\mu\left[2\frac{\partial\mathbf{v}_{\mathrm{r}}}{\partial \mathrm{r}}-\frac{2}{3}\left(\nabla\cdot\mathbf{v}\right)\right]\\\boldsymbol{\tau}_{\varphi\varphi}&=-\mu\left[2\left(\frac{1}{\mathrm{r}}\frac{\partial\mathbf{v}_{\varphi}}{\partial\varphi}+\frac{\mathbf{v}_{\mathrm{r}}}{\mathrm{r}}\right)-\frac{2}{3}\left(\nabla\cdot\mathbf{v}\right)\right]\\\boldsymbol{\tau}_{zz}&=-\mu\left[2\frac{\partial\mathbf{v}_{z}}{\partial \mathrm{z}}-\frac{2}{3}\left(\nabla\cdot\mathbf{v}\right)\right]\\\boldsymbol{\tau}_{\mathrm{r}\varphi}&=\tau_{\varphi\mathrm{r}}=-\mu\left[\mathrm{r}\frac{\partial}{\partial \mathrm{r}}\left(\frac{\mathbf{v}_{\varphi}}{\mathrm{r}}\right)+\frac{1}{\mathrm{r}}\frac{\partial\mathbf{v}_{\mathrm{r}}}{\partial\varphi}\right]\\\boldsymbol{\tau}_{z\varphi}&=\tau_{\varphi z}=-\mu\left[\frac{\partial\mathbf{v}_{\varphi}}{\partial \mathrm{z}}+\frac{1}{\mathrm{r}}\frac{\partial\mathbf{v}_{z}}{\partial\varphi}\right]\\\boldsymbol{\tau}_{zr}&=\tau_{\mathrm{r}z}=-\mu\left[\frac{\partial\mathbf{v}_{z}}{\partial r}+\frac{\partial\mathbf{v}_{\mathrm{r}}}{\partial \mathrm{z}}\right]\end{aligned}\tag{3.29}$$

r-component

$$\begin{aligned}
&\frac{\partial}{\partial t}\left(\mathbf{v}_{\mathrm{r}}\rho\right)+\mathbf{v}_{\mathrm{r}}\frac{\partial}{\partial r}\left(\rho\mathbf{v}_{\mathrm{r}}\right)+\frac{\mathbf{v}_{\varphi}}{\mathrm{r}}\frac{\partial}{\partial\varphi}\left(\rho\mathbf{v}_{\mathrm{r}}\right)-\frac{\left(\mathbf{v}_{\varphi}\right)^{2}}{\mathrm{r}}+\mathbf{v}_{\mathrm{z}}\frac{\partial}{\partial\mathrm{z}}\left(\rho\mathbf{v}_{\mathrm{r}}\right)\\
&\quad=\frac{\rho g_{\mathrm{r}}}{\eta\theta}-\frac{1}{\eta\theta}\left\{\frac{1}{\mathrm{r}}\frac{\partial}{\partial\mathrm{r}}\left(\mathrm{rP}_{\mathrm{r}}\right)\right\}+\mu\eta\theta\left\{\frac{1}{\mathrm{r}}\frac{\partial}{\partial\mathrm{r}}\left(\mathrm{r}\left[2\frac{\partial\mathbf{v}_{\mathrm{r}}}{\partial\mathrm{r}}-\frac{2}{3}\left(\nabla\cdot\mathbf{v}\right)\right]\right)\right.\\
&\quad+\frac{1}{\mathrm{r}}\frac{\partial}{\partial\varphi}\left(\left[\mathrm{r}\frac{\partial}{\partial\mathrm{r}}\left(\frac{\mathbf{v}_{\varphi}}{\mathrm{r}}\right)+\frac{1}{\mathrm{r}}\frac{\partial\mathbf{v}_{\mathrm{r}}}{\partial\varphi}\right]\right)-\frac{1}{\mathrm{r}}\left[2\left(\frac{1}{\mathrm{r}}\frac{\partial\mathbf{v}_{\varphi}}{\partial\varphi}+\frac{\mathbf{v}_{\mathrm{r}}}{\mathrm{r}}\right)-\frac{2}{3}\left(\nabla\cdot\mathbf{v}\right)\right]\\
&\quad\left.+\frac{\partial}{\partial\mathrm{z}}\left(\left[\frac{\partial\mathbf{v}_{\mathrm{z}}}{\partial\mathrm{r}}+\frac{\partial\mathbf{v}_{\mathrm{r}}}{\partial\mathrm{z}}\right]\right)\right\}
\end{aligned}\tag{3.30}$$

φ -component

$$\begin{aligned}
&\frac{\partial}{\partial t}\left(\mathbf{v}_{\varphi}\rho\right)+\mathbf{v}_{\mathrm{r}}\frac{\partial}{\partial\mathrm{r}}\left(\rho\mathbf{v}_{\varphi}\right)+\frac{\mathbf{v}_{\varphi}}{\mathrm{r}}\frac{\partial}{\partial\varphi}\left(\rho\mathbf{v}_{\varphi}\right)+\frac{\mathbf{v}_{\mathrm{r}}\mathbf{v}_{\varphi}}{\mathrm{r}}+\mathbf{v}_{\mathrm{z}}\frac{\partial}{\partial\mathrm{z}}\left(\rho\mathbf{v}_{\varphi}\right)\\
&\quad=\frac{\rho g_{\varphi}}{\eta\theta}-\frac{1}{\eta\theta}\left\{\frac{1}{\mathrm{r}}\frac{\partial\mathrm{P}_{\varphi}}{\partial\varphi}\right\}+\mu\eta\theta\left\{\frac{1}{\mathrm{r}^{2}}\frac{\partial}{\partial\mathrm{r}}\left(\mathrm{r}^{2}\left[\mathrm{r}\frac{\partial}{\partial\mathrm{r}}\left(\frac{\mathbf{v}_{\varphi}}{\mathrm{r}}\right)+\frac{1}{\mathrm{r}}\frac{\partial\mathbf{v}_{\mathrm{r}}}{\partial\varphi}\right]\right)\right.\\
&\quad\left.+\frac{1}{\mathrm{r}}\frac{\partial}{\partial\varphi}\left(\left[2\left(\frac{1}{\mathrm{r}}\frac{\partial\mathbf{v}_{\varphi}}{\partial\varphi}+\frac{\mathbf{v}_{\mathrm{r}}}{\mathrm{r}}\right)-\frac{2}{3}\left(\nabla\cdot\mathbf{v}\right)\right]\right)+\frac{\partial}{\partial\mathrm{z}}\left(\left[\frac{\partial\mathbf{v}_{\varphi}}{\partial\mathrm{z}}+\frac{1}{\mathrm{r}}\frac{\partial\mathbf{v}_{\mathrm{z}}}{\partial\varphi}\right]\right)\right\}
\end{aligned}\tag{3.31}$$

z-component

$$\begin{aligned}
&\frac{\partial}{\partial t}\left(\mathbf{v}_{\mathrm{z}}\rho\right)+\mathbf{v}_{\mathrm{r}}\frac{\partial}{\partial\mathrm{r}}\left(\rho\mathbf{v}_{\mathrm{z}}\right)+\frac{\mathbf{v}_{\varphi}}{\mathrm{r}}\frac{\partial}{\partial\varphi}\left(\rho\mathbf{v}_{\mathrm{z}}\right)+\mathbf{v}_{\mathrm{z}}\frac{\partial}{\partial\mathrm{z}}\left(\rho\mathbf{v}_{\mathrm{z}}\right)\\
&\quad=\frac{\rho g_{\mathrm{z}}}{\eta\theta}-\frac{1}{\eta\theta}\left\{\frac{\partial\mathrm{P}_{\mathrm{z}}}{\partial\mathrm{z}}\right\}+\mu\eta\theta\left\{\frac{1}{\mathrm{r}}\frac{\partial}{\partial\mathrm{r}}\left(\mathrm{r}\left[\frac{\partial\mathbf{v}_{\mathrm{z}}}{\partial\mathrm{r}}+\frac{\partial\mathbf{v}_{\mathrm{r}}}{\partial\mathrm{z}}\right]\right)\right.\\
&\quad\left.+\frac{1}{\mathrm{r}}\frac{\partial}{\partial\varphi}\left(\left[\frac{\partial\mathbf{v}_{\varphi}}{\partial\mathrm{z}}+\frac{1}{\mathrm{r}}\frac{\partial\mathbf{v}_{\mathrm{z}}}{\partial\varphi}\right]\right)+\frac{\partial}{\partial\mathrm{z}}\left(\left[2\frac{\partial\mathbf{v}_{\mathrm{z}}}{\partial\mathrm{z}}-\frac{2}{3}\left(\nabla\cdot\mathbf{v}\right)\right]\right)\right\}
\end{aligned}\tag{3.32}$$

The indicated differentiations in (3.30), (3.31), and (3.32) are performed and each equation is rewritten for a multicomponent multiphase system. Thus, the governing equations for conservation of momentum are

r-component

$$\frac{\partial}{\partial t}\left(\rho_{\alpha,\beta}\mathbf{v}_{r_{\alpha,\beta}}\right)+\mathbf{v}_{r_{\alpha,\beta}}\frac{\partial}{\partial r}\left(\rho_{\alpha,\beta}\mathbf{v}_{r_{\alpha,\beta}}\right)+\frac{\mathbf{v}_{\varphi_{\alpha,\beta}}}{r}\frac{\partial}{\partial \varphi}\left(\rho_{\alpha,\beta}\mathbf{v}_{r_{\alpha,\beta}}\right)-\frac{\left(\mathbf{v}_{\varphi_{\alpha,\beta}}\right)^2}{r}+\mathbf{v}_{z_{\alpha,\beta}}\frac{\partial}{\partial z}\left(\rho_{\alpha,\beta}\mathbf{v}_{r_{\alpha,\beta}}\right)$$
$$=\frac{\rho_{\alpha,\beta}g}{\eta\theta_{\alpha,\beta}}-\frac{1}{\eta\theta_{\alpha,\beta}}\left\{\frac{1}{r}\frac{\partial}{\partial r}\left(rP_{r_{\alpha,\beta}}\right)\right\}+\mu_{\alpha,\beta}\eta\theta_{\alpha,\beta}\left\{\frac{\partial}{\partial r}\left[\frac{1}{r}\frac{\partial}{\partial r}\left(r\mathbf{v}_{r_{\alpha,\beta}}\right)\right]\right. \tag{3.33}$$
$$\left.+\frac{1}{r^2}\frac{\partial^2\mathbf{v}_{r_{\alpha,\beta}}}{\partial\varphi^2}-\frac{2}{r^2}\frac{\partial\mathbf{v}_{\varphi_{\alpha,\beta}}}{\partial\varphi}+\left(\frac{\partial^2\mathbf{v}_{r_{\alpha,\beta}}}{\partial z^2}\right)+\frac{2}{3r}\left(\nabla\cdot\mathbf{v}_{\alpha,\beta}\right)-\frac{2}{3}\frac{\partial}{\partial r}\left(\nabla\cdot\mathbf{v}_{\alpha,\beta}\right)\right\}$$

φ -component

$$\frac{\partial}{\partial t}\left(\rho_{\alpha,\beta}\mathbf{v}_{\varphi_{\alpha,\beta}}\right)+\mathbf{v}_{r_{\alpha,\beta}}\frac{\partial}{\partial r}\left(\rho_{\alpha,\beta}\mathbf{v}_{\varphi_{\alpha,\beta}}\right)+\frac{\mathbf{v}_{\varphi_{\alpha,\beta}}}{r}\frac{\partial}{\partial \varphi}\left(\rho_{\alpha,\beta}\mathbf{v}_{\varphi_{\alpha,\beta}}\right)+\frac{\mathbf{v}_{r_{\alpha,\beta}}\mathbf{v}_{\varphi_{\alpha,\beta}}}{r}+\mathbf{v}_{z_{\alpha,\beta}}\frac{\partial}{\partial z}\left(\rho_{\alpha,\beta}\mathbf{v}_{\varphi}\right)$$
$$=\frac{\rho_{\alpha,\beta}g}{\eta\theta_{\alpha,\beta}}-\frac{1}{\eta\theta_{\alpha,\beta}}\left\{\frac{1}{r}\frac{\partial P_{\varphi_{\alpha,\beta}}}{\partial\varphi}\right\}+\mu_{\alpha,\beta}\eta\theta_{\alpha,\beta}\left\{\frac{\partial^2\mathbf{v}_{\varphi_{\alpha,\beta}}}{\partial r^2}-\left(\frac{\mathbf{v}_{\varphi_{\alpha,\beta}}}{r^2}\right)+\frac{\partial\mathbf{v}_{\varphi_{\alpha,\beta}}}{\partial r}\right. \tag{3.34}$$
$$\left.+\frac{2}{r^2}\frac{\partial^2\mathbf{v}_{\varphi_{\alpha,\beta}}}{\partial\varphi^2}+\frac{2}{r^2}\frac{\partial\mathbf{v}_{r_{\alpha,\beta}}}{\partial\varphi}+\frac{\partial^2\mathbf{v}_{\varphi_{\alpha,\beta}}}{\partial z^2}-\frac{2}{3r}\frac{\partial}{\partial\varphi}\left(\nabla\cdot\mathbf{v}_{\alpha,\beta}\right)\right\}$$

z-component

$$\frac{\partial}{\partial t}\left(\rho_{\alpha,\beta}\mathbf{v}_{z_{\alpha,\beta}}\right)+\mathbf{v}_{r_{\alpha,\beta}}\frac{\partial}{\partial r}\left(\rho_{\alpha,\beta}\mathbf{v}_{z_{\alpha,\beta}}\right)+\frac{\mathbf{v}_{\varphi_{\alpha,\beta}}}{r}\frac{\partial}{\partial \varphi}\left(\rho_{\alpha,\beta}\mathbf{v}_{z_{\alpha,\beta}}\right)+\mathbf{v}_{z_{\alpha,\beta}}\frac{\partial}{\partial z}\left(\rho_{\alpha,\beta}\mathbf{v}_{z_{\alpha,\beta}}\right)$$
$$=\frac{\rho_{\alpha,\beta}g}{\eta\theta_{\alpha,\beta}}-\frac{1}{\eta\theta_{\alpha,\beta}}\left\{\frac{\partial P_{z_{\alpha,\beta}}}{\partial z}\right\}+\mu_{\alpha,\beta}\eta\theta_{\alpha,\beta}\left\{\frac{1}{r}\frac{\partial}{\partial r}\left(r\frac{\partial\mathbf{v}_{z_{\alpha,\beta}}}{\partial r}\right)\right. \tag{3.35}$$
$$\left.+\frac{1}{r^2}\frac{\partial^2\mathbf{v}_{z_{\alpha,\beta}}}{\partial\varphi^2}+\frac{\partial^2\mathbf{v}_{z_{\alpha,\beta}}}{\partial z^2}-\frac{2}{3}\frac{\partial}{\partial z}\left(\nabla\cdot\mathbf{v}_{\alpha,\beta}\right)\right\}$$

Since the liquid phase is assumed to be immobile in this system, the equations for conservation of momentum are written only for the gas phase for the components TCE, air, and water as a single miscible phase (i.e., ideal gas).

r-component

$$\frac{\partial}{\partial t}\left(\rho_{g;TCE,N_2,water}\mathbf{v}_{r_{g;TCE,N_2,water}}\right)+\mathbf{v}_{r_{g;TCE,N_2,water}}\frac{\partial}{\partial r}\left(\rho_{g;TCE,N_2,water}\mathbf{v}_{r_{g;TCE,N_2,water}}\right)$$
$$+\frac{\mathbf{v}_{\varphi_{g;TCE,N_2,water}}}{r}\frac{\partial}{\partial\varphi}\left(\rho_{g;TCE,N_2,water}\mathbf{v}_{r_{g;TCE,N_2,water}}\right)-\frac{\left(\mathbf{v}_{\varphi_{g;TCE,N_2,water}}\right)^2}{r}$$
$$+\mathbf{v}_{z_{g;TCE,N_2,water}}\frac{\partial}{\partial z}\left(\rho_{g;TCE,N_2,water}\mathbf{v}_{r_{g;TCE,N_2,water}}\right)=\frac{\rho_{g;TCE,N_2,water}g}{\eta\theta_{g;TCE,N_2,water}}$$
$$-\frac{1}{\eta\theta_{g;TCE,N_2,water}}\left\{\frac{1}{r}\frac{\partial}{\partial r}\left(rP_{r_{g;TCE,N_2,water}}\right)\right\}$$
$$+\mu_{g;TCE,N_2,water}\eta\theta_{g;TCE,N_2,water}\left\{\frac{\partial}{\partial r}\left[\frac{1}{r}\frac{\partial}{\partial r}\left(r\mathbf{v}_{r_{g;TCE,N_2,water}}\right)\right]\right.$$
$$+\frac{1}{r^2}\frac{\partial^2\mathbf{v}_{r_{g;TCE,N_2,water}}}{\partial\varphi^2}-\frac{2}{r^2}\frac{\partial\mathbf{v}_{\varphi_{g;TCE,N_2,water}}}{\partial\varphi}+\left(\frac{\partial^2\mathbf{v}_{r_{g;TCE,N_2,water}}}{\partial z^2}\right)$$
$$\left.+\frac{2}{3r}\left(\nabla\cdot\mathbf{v}_{g;TCE,N_2,water}\right)-\frac{2}{3}\frac{\partial}{\partial r}\left(\nabla\cdot\mathbf{v}_{g;TCE,N_2,water}\right)\right\} \tag{3.36}$$

φ -component

$$\frac{\partial}{\partial t}\left(\rho_{g;TCE,N_2,water}\mathbf{v}_{\varphi_{g;TCE,N_2,water}}\right)+\mathbf{v}_{r_{g;TCE,N_2,water}}\frac{\partial}{\partial r}\left(\rho_{g;TCE,N_2,water}\mathbf{v}_{\varphi_{g;TCE,N_2,water}}\right)$$
$$+\frac{\mathbf{v}_{\varphi_{g;TCE,N_2,water}}}{r}\frac{\partial}{\partial\varphi}\left(\rho_{g;TCE,N_2,water}\mathbf{v}_{\varphi_{g;TCE,N_2,water}}\right)+\frac{\mathbf{v}_{r_{g;TCE,N_2,water}}\mathbf{v}_{\varphi_{g;TCE,N_2,water}}}{r}$$
$$+\mathbf{v}_{z_{g;TCE,N_2,water}}\frac{\partial}{\partial z}\left(\rho_{g;TCE,N_2,water}\mathbf{v}_{\varphi_{g;TCE,N_2,water}}\right)=\frac{\rho_{g;TCE,N_2,water}g}{\eta\theta_{g;TCE,N_2,water}}$$
$$-\frac{1}{\eta\theta_{g;TCE,N_2,water}}\left\{\frac{1}{r}\frac{\partial P_{\varphi_{g;TCE,N_2,water}}}{\partial\varphi}\right\}$$
$$+\mu_{g;TCE,N_2,water}\eta\theta_{g;TCE,N_2,water}\left\{\frac{\partial^2\mathbf{v}_{\varphi_{g;TCE,N_2,water}}}{\partial r^2}\right.$$
$$-\left(\frac{\mathbf{v}_{\varphi_{g;TCE,N_2,water}}}{r^2}\right)+\frac{\partial\mathbf{v}_{\varphi_{g;TCE,N_2,water}}}{\partial r}+\frac{2}{r^2}\frac{\partial^2\mathbf{v}_{\varphi_{g;TCE,N_2,water}}}{\partial\varphi^2}$$
$$\left.+\frac{2}{r^2}\frac{\partial\mathbf{v}_{r_{g;TCE,N_2,water}}}{\partial\varphi}+\frac{\partial^2\mathbf{v}_{\varphi_{g;TCE,N_2,water}}}{\partial z^2}-\frac{2}{3r}\frac{\partial}{\partial\varphi}\left(\nabla\cdot\mathbf{v}_{g;TCE,N_2,water}\right)\right\} \tag{3.37}$$

z-component

$$\frac{\partial}{\partial t}\left(\rho_{g;TCE,N_2,water}\mathbf{v}_{z_{g;TCE,N_2,water}}\right)+\mathbf{v}_{r_{g;TCE,N_2,water}}\frac{\partial}{\partial r}\left(\rho_{g;TCE,N_2,water}\mathbf{v}_{z_{g;TCE,N_2,water}}\right)$$
$$+\frac{\mathbf{v}_{\varphi_{g;TCE,N_2,water}}}{r}\frac{\partial}{\partial \varphi}\left(\rho_{g;TCE,N_2,water}\mathbf{v}_{z_{g;TCE,N_2,water}}\right)+\mathbf{v}_{z_{g;TCE,N_2,water}}\frac{\partial}{\partial z}\left(\rho_{g;TCE,N_2,water}\mathbf{v}_{z_{g;TCE,N_2,water}}\right)$$
$$=\frac{\rho_{g;TCE,N_2,water}g}{\eta\theta_{g;TCE,N_2,water}}-\frac{1}{\eta\theta_{g;TCE,N_2,water}}\left\{\frac{\partial P_{z_{g;TCE,N_2,water}}}{\partial z}\right\} \tag{3.38}$$
$$+\mu_{g;TCE,N_2,water}\eta\theta_{g;TCE,N_2,water}\left\{\frac{1}{r}\frac{\partial}{\partial r}\left(r\frac{\partial \mathbf{v}_{z_{g;TCE,N_2,water}}}{\partial r}\right)+\frac{1}{r^2}\frac{\partial^2\mathbf{v}_{z_{g;TCE,N_2,water}}}{\partial\varphi^2}\right.$$
$$\left.+\frac{\partial^2\mathbf{v}_{z_{g;TCE,N_2,water}}}{\partial z^2}-\frac{2}{3}\frac{\partial}{\partial z}\left(\nabla\cdot\mathbf{v}_{g;TCE,N_2,water}\right)\right\}$$

3.2.3 Conservation of Energy

The governing conservation of energy equation is derived from the Reynolds Transport Theorem

$$\frac{\partial}{\partial t}\iiint_{CV}\hat{U}\boldsymbol{\rho}\,dV+\iint_{CS}\hat{U}\boldsymbol{\rho}(\mathbf{v}\cdot n)\,dA+\iint_{CS}\mathbf{q}\,dA+\iint_{CS}P(\mathbf{v}\cdot n)\,dA+\iint_{CV}Q\,dV=0 \tag{3.39}$$

The necessary integrations are performed over the differential control volume (Figure 3.3) and control surface (Figures 3.1).

$$\frac{\partial}{\partial t}U\boldsymbol{\rho}V+U\boldsymbol{\rho}\left(-\mathbf{v}_aA_a+\mathbf{v}_bA_b-\mathbf{v}_cA_c+\mathbf{v}_dA_d-\mathbf{v}_eA_e+\mathbf{v}_fA_f\right)$$
$$+\mathbf{q}\left(A_a+A_b-A_c+A_d-A_e+A_f\right) \tag{3.40}$$
$$+P\left(-\mathbf{v}_aA_a+\mathbf{v}_bA_b-\mathbf{v}_cA_c+\mathbf{v}_dA_d-\mathbf{v}_eA_e+\mathbf{v}_fA_f\right)+QV=0$$

Volume, area and velocity components (Table 3.1) may be substituted into the above equation

$$\begin{aligned}
&\frac{\partial}{\partial t}\left(\mathrm{U}\boldsymbol{\rho}\theta\eta r\Delta r\Delta\varphi\Delta z\right)+\mathrm{U}\boldsymbol{\rho}\left\{\Delta r\Delta z\eta\theta\left[\left(\mathbf{v}_{\phi}+\frac{\partial\mathbf{v}_{\phi}}{\partial\phi}\right)-\mathbf{v}_{\phi}\right]\right.\\
&\quad+\Delta\varphi\Delta z\eta\theta\left[\left(\mathrm{r}+\Delta\mathrm{r}\right)\left(\mathbf{v}_{r}+\frac{\partial\mathbf{v}_{r}}{\partial r}\right)-r\mathbf{v}_{r}\right]+\mathrm{r}\Delta r\Delta\varphi\eta\theta\left[\left(\mathbf{v}_{z}+\frac{\partial\mathbf{v}_{z}}{\partial z}\right)-\mathbf{v}_{z}\right]\Bigg\}\\
&\quad+\left\{\Delta r\Delta z\eta\theta\left[\left(\mathbf{q}_{\phi}+\frac{\partial\mathbf{q}_{\phi}}{\partial\phi}\right)-\mathbf{q}_{\phi}\right]+\Delta\varphi\Delta z\eta\theta\left[\left(\mathrm{r}+\Delta\mathrm{r}\right)\left(\mathbf{q}_{r}+\frac{\partial\mathbf{q}_{r}}{\partial r}\right)-r\mathbf{v}_{r}\right]\right.\\
&\quad+\mathrm{r}\Delta r\Delta\varphi\eta\theta\left[\left(\mathbf{q}_{z}+\frac{\partial\mathbf{q}_{z}}{\partial z}\right)-\mathbf{q}_{z}\right]\Bigg\}\\
&\quad+\mathrm{P}\left\{\Delta r\Delta z\eta\theta\left[\left(\mathbf{v}_{\phi}+\frac{\partial\mathbf{v}_{\phi}}{\partial\phi}\right)-\mathbf{v}_{\phi}\right]+\Delta\varphi\Delta z\eta\theta\left[\left(\mathrm{r}+\Delta\mathrm{r}\right)\left(\mathbf{v}_{r}+\frac{\partial\mathbf{v}_{r}}{\partial r}\right)-r\mathbf{v}_{r}\right]\right.\\
&\quad+\mathrm{r}\Delta r\Delta\varphi\eta\theta\left[\left(\mathbf{v}_{z}+\frac{\partial\mathbf{v}_{z}}{\partial z}\right)-\mathbf{v}_{z}\right]\Bigg\}+\mathrm{Q}\theta\eta r\Delta r\Delta\varphi\Delta z=0
\end{aligned}\tag{3.41}$$

Dividing (3.41) by $\left(\eta\theta r\Delta r\Delta\varphi\Delta z\right)$

$$\begin{aligned}
&\frac{\partial}{\partial t}\left(\mathrm{U}\boldsymbol{\rho}\right)+\mathrm{U}\boldsymbol{\rho}\left\{\frac{1}{\mathrm{r}\Delta\varphi}\left[\left(\mathbf{v}_{\varphi}+\frac{\partial\mathbf{v}_{\varphi}}{\partial\varphi}\right)-\mathbf{v}_{\varphi}\right]+\frac{1}{\mathrm{r}\Delta\mathrm{r}}\left[\left(\mathrm{r}+\Delta\mathrm{r}\right)\left(\mathbf{v}_{\mathrm{r}}+\frac{\partial\mathbf{v}_{\mathrm{r}}}{\partial\mathrm{r}}\right)-\mathrm{r}\mathbf{v}_{r}\right]\right.\\
&\quad+\frac{1}{\Delta\mathrm{z}}\left[\left(\mathbf{v}_{\mathrm{z}}+\frac{\partial\mathbf{v}_{\mathrm{z}}}{\partial\mathrm{z}}\right)-\mathbf{v}_{\mathrm{z}}\right]\Bigg\}+\left\{\frac{1}{\mathrm{r}\Delta\varphi}\left[\left(\mathbf{q}_{\varphi}+\frac{\partial\mathbf{q}_{\varphi}}{\partial\varphi}\right)-\mathbf{q}_{\varphi}\right]\right.\\
&\quad+\frac{1}{\mathrm{r}\Delta\mathrm{r}}\left[\left(\mathrm{r}+\Delta\mathrm{r}\right)\left(\mathbf{q}_{\mathrm{r}}+\frac{\partial\mathbf{q}_{\mathrm{r}}}{\partial\mathrm{r}}\right)-\mathrm{r}\mathbf{v}_{\mathrm{r}}\right]+\frac{1}{\Delta\mathrm{z}}\left[\left(\mathbf{q}_{\mathrm{z}}+\frac{\partial\mathbf{q}_{\mathrm{z}}}{\partial\mathrm{z}}\right)-\mathbf{q}_{\mathrm{z}}\right]\Bigg\}\\
&\quad+\mathrm{P}\left\{\frac{1}{\mathrm{r}\Delta\varphi}\left[\left(\mathbf{v}_{\varphi}+\frac{\partial\mathbf{v}_{\varphi}}{\partial\varphi}\right)-\mathbf{v}_{\varphi}\right]+\frac{1}{\mathrm{r}\Delta\mathrm{r}}\left[\left(\mathrm{r}+\Delta\mathrm{r}\right)\left(\mathbf{v}_{\mathrm{r}}+\frac{\partial\mathbf{v}_{\mathrm{r}}}{\partial\mathrm{r}}\right)-\mathrm{r}\mathbf{v}_{\mathrm{r}}\right]\right.\\
&\quad+\frac{1}{\Delta\mathrm{z}}\left[\left(\mathbf{v}_{\mathrm{z}}+\frac{\partial\mathbf{v}_{\mathrm{z}}}{\partial\mathrm{z}}\right)-\mathbf{v}_{\mathrm{z}}\right]\Bigg\}+\mathrm{Q}=0
\end{aligned}\tag{3.42}$$

The simplest form of the conservation of energy equation is achieved by taking the limit of (3.42) as r, φ, and z approach zero and rewriting the equation in tensor notation.

$$\frac{\partial}{\partial t}\left(\boldsymbol{\rho}\hat{\mathrm{U}}\right) = -\left(\nabla\cdot\rho\mathbf{v}\hat{\mathrm{U}}\right) - \left(\nabla\cdot\mathbf{q}\right) - \left(\nabla\cdot\mathrm{P}\mathbf{v}\right) + \mathrm{Q} \tag{3.43}$$

This relationship can be simplified further using Fourier's Law. Therefore, the general multiphase multicomponent energy equation is

$$\frac{\partial}{\partial t}\left(\boldsymbol{\rho}_{\alpha,\beta}\hat{\mathrm{U}}_{\alpha,\beta}\right) = -\left(\nabla\cdot\rho_{\alpha,\beta}\mathbf{v}_{\alpha,\beta}\hat{\mathrm{U}}_{\alpha,\beta}\right) - \left(k\nabla^2\mathrm{T}\right) - \left(\nabla\cdot\mathrm{P}\mathbf{v}_{\alpha,\beta}\right) + \mathrm{Q} \tag{3.44}$$

For the components TCE, air, and water, the equation for conservation of energy in the gas phase is:

$$\begin{aligned}\frac{\partial}{\partial t}&\left(\boldsymbol{\rho}_{g;TCE,N_2,water}\hat{\mathrm{U}}_{g;TCE,N_2,water}\right)\\ &= -\left(\nabla\cdot\rho_{g;TCE,N_2,water}\mathbf{v}_{g;TCE,N_2,water}\hat{\mathrm{U}}_{g;TCE,N_2,water}\right)\\ &\quad -\left(k\nabla^2\mathrm{T}\right) - \left(\nabla\cdot\mathrm{P}\mathbf{v}_{g;TCE,N_2,water}\right) + \mathrm{Q}\end{aligned} \tag{3.45}$$

Since the liquid phase is immobile in this system ($\mathbf{v}_l = 0$), conservation of energy is written as:

$$\frac{\partial}{\partial t}\left(\boldsymbol{\rho}_{l;TCE,N_2,water}\hat{\mathrm{U}}_{l;TCE,N_2,water}\right) = -\left(k\nabla^2\mathrm{T}\right) + \mathrm{Q} \tag{3-46}$$

3.3 Methodology for Model Solution

The set of governing equations (3.8, 3.9, 3.36, 3.37, 3.38, 3.45 and 3.46) can be solved simultaneous using a number of applicable numerical methods, such as finite element or finite volume techniques. All variables of each equation are known except $\mathbf{q}, \hat{U}$, and $\mathbf{v}$. Appendix A lists known relationships for saturation, porosity, moisture content, specific heat, enthalpy, internal energy and relationships derived from the ideal gas law that will aid in model solution.

CHAPTER IV

SUMMARY AND CONCLUSIONS

Thermally enhanced soil vapor extraction (SVE) has become a recognized technique for subsurface remediation of both volatile organic compounds (VOCs) and contaminants traditionally too non-volatile to implement SVE. Thermal enhancement extends the range of soil types where traditional SVE can be used. Although thermally enhanced SVE has become popular in recent years, few approaches characterize the system conceptually and mathematically on the basis of conservation of mass, momentum and energy. A set of governing equations were written for a general multiphase, multicomponent system with an applied heat flux. Any equation can be written in a more specific manner to more accurately describe the system being studied. This general approach allows the set of governing equation to be applied to any thermal treatment with an applied heat flux.

Deriving the conservation equations followed the shell balance method of Bird, Stewart and Lightfoot (1960). Appropriate simplifying assumptions were made, such as local thermal equilibrium, to formulate the conservation equations. It was beyond the scope of this work to solve the set of governing equations. The equations can be solved simultaneously with a finite element package, such as ABAQUS, for a theoretical situation using typical values found in the literature. Much more detailed research is needed regarding phase transitions, especially the evaporation/condensation process before the mechanisms of thermally enhanced SVE can be fully understood.

Appendices

APPENDIX A: KNOWN RELATIONSHIPS

Porosity, Saturation and Moisture Content Relationships

$$S_{\alpha,\beta} = \frac{\theta_{\alpha,\beta}}{\eta} \quad \text{A-1}$$

$$\theta_{l,total} = \theta_{l,water} + \theta_{l,NAPL} \quad \text{A-2}$$

$$\theta_{g,total} = \theta_{g,water} + \theta_{g,NAPL} \quad \text{A-3}$$

$$\theta_{g,total} = 1 - \theta_{l,total} \quad \text{A-4}$$

$$S_{g,total} = \frac{\theta_{g,total}}{\eta} \quad \text{A-5}$$

$$S_{g,total} = \frac{\theta_{g,water} + \theta_{g,NAPL}}{\eta} \quad \text{A-6}$$

$$S_{g,total} = \frac{1 - \theta_{l,total}}{\eta} \quad \text{A-7}$$

$$S_{g,total} = \frac{1 - \left(\theta_{l,water} + \theta_{l,NAPL}\right)}{\eta} \quad \text{A-8}$$

$$S_{l,total} = \frac{\theta_{l,total}}{\eta} \quad \text{A-9}$$

$$S_{l,total} = \frac{\theta_{l,total}}{\eta} \quad \text{A-10}$$

$$S_{l,total} = \frac{\theta_{l,water} + \theta_{l,NAPL}}{\eta} \quad \text{A-11}$$

Ideal Gas Law Relationship

$$\rho_{\alpha,\beta} = \frac{m_{\alpha,\beta}}{V} = \frac{M_w n_{\alpha,\beta}}{V} = \frac{M_{w_\beta}}{R}\frac{P}{T} \qquad \text{A-12}$$

Specific Heat, Enthalpy, Internal Energy Relationships

$$\left(\frac{\partial \hat{U}_\alpha}{\partial t}\right)_V = C_{V_\alpha} \qquad \text{A-13}$$

$$\left(\frac{\partial \hat{H}_\alpha}{\partial t}\right)_P = C_{P_\alpha} \qquad \text{A-14}$$

$$C_V = C_P + R \qquad \text{A-15}$$

$$\hat{U} = \hat{H} - P\hat{V} \qquad \text{A-16}$$

$$\frac{\partial \hat{U}}{\partial t} = \frac{\partial \hat{H}}{\partial t} - \left(P\frac{\partial \hat{V}}{\partial t} + \hat{V}\frac{\partial P}{\partial t}\right) \qquad \text{A-17}$$

$$\hat{H} = \int_{T_{ref}}^{T} C_P \, dT \qquad \text{A-18}$$

$$\hat{U} = \int_{T_{ref}}^{T} C_V \, dT \qquad \text{A-19}$$

$$\hat{U} = \int_{T_{ref}}^{T} C_p dT + R\int_{T_{ref}}^{T} dT \qquad \text{A-20}$$

$$\int_{T_{ref}}^{T} C_V \, dT = C_P(T - T_{ref}) + R(T - T_{ref}) \qquad \text{A-21}$$

$$\hat{H}=\int_{T_{ref_l}}^{T_l} C_{P_l}\ dT+\Delta\hat{H}_{vap}+\int_{T_{ref_g}}^{T_g} C_{P_g}\ dT \qquad \text{A-22}$$

$$\hat{U}=\int_{T_{ref_l}}^{T_l} C_{P_l}\ dT+\Delta\hat{H}_{vap}+\int_{T_{ref_g}}^{T_g} C_{P_g}\ dT - PV \qquad \text{A-23}$$

APPENDIX B: GOVERNING EQUATIONS (SUMMARIZED)

Conservation of Mass

(gas phase)

$$\frac{\partial}{\partial t}\eta\theta_{g;TCE,\,N_2,water}\rho_{g;TCE,\,N_2,water}+(\nabla\cdot\rho_{g;TCE,\,N_2,water}\mathbf{v}_{g;TCE,\,N_2,water})=\pm\frac{\mathbf{q}}{h_{vap}} \qquad \text{B-1}$$

(liquid phase)

$$\backslash\frac{\partial}{\partial t}\eta\theta_{l;TCE,\,N_2,water}\rho_{l;TCE,\,N_2,water}=\pm\frac{\mathbf{q}}{h_{vap}} \qquad \text{B-2}$$

Conservation of Momentum

(gas phase only)

r-component

$$\begin{aligned}
&\frac{\partial}{\partial t}\left(\rho_{g;TCE,N_2,water}\mathbf{v}_{r_{g;TCE,N_2,water}}\right)+\mathbf{v}_{r_{g;TCE,N_2,water}}\frac{\partial}{\partial r}\left(\rho_{g;TCE,N_2,water}\mathbf{v}_{r_{g;TCE,N_2,water}}\right)\\
&\quad+\frac{\mathbf{v}_{\varphi_{g;TCE,N_2,water}}}{r}\frac{\partial}{\partial\varphi}\left(\rho_{g;TCE,N_2,water}\mathbf{v}_{r_{g;TCE,N_2,water}}\right)-\frac{\left(\mathbf{v}_{\varphi_{g;TCE,N_2,water}}\right)^2}{r}\\
&\quad+\mathbf{v}_{z_{g;TCE,N_2,water}}\frac{\partial}{\partial z}\left(\rho_{g;TCE,N_2,water}\mathbf{v}_{r_{g;TCE,N_2,water}}\right)=\frac{\rho_{g;TCE,N_2,water}g}{\eta\theta_{g;TCE,N_2,water}}\\
&\quad-\frac{1}{\eta\theta_{g;TCE,N_2,water}}\left\{\frac{1}{r}\frac{\partial}{\partial r}\left(rP_{r_{g;TCE,N_2,water}}\right)\right\}\\
&\quad+\mu_{g;TCE,N_2,water}\eta\theta_{g;TCE,N_2,water}\left\{\frac{\partial}{\partial r}\left[\frac{1}{r}\frac{\partial}{\partial r}\left(r\mathbf{v}_{r_{g;TCE,N_2,water}}\right)\right]\right.\\
&\quad+\frac{1}{r^2}\frac{\partial^2\mathbf{v}_{r_{g;TCE,N_2,water}}}{\partial\varphi^2}-\frac{2}{r^2}\frac{\partial\mathbf{v}_{\varphi_{g;TCE,N_2,water}}}{\partial\varphi}+\left(\frac{\partial^2\mathbf{v}_{r_{g;TCE,N_2,water}}}{\partial z^2}\right)\\
&\quad\left.+\frac{2}{3r}\left(\nabla\cdot\mathbf{v}_{g;TCE,N_2,water}\right)-\frac{2}{3}\frac{\partial}{\partial r}\left(\nabla\cdot\mathbf{v}_{g;TCE,N_2,water}\right)\right\}
\end{aligned} \qquad \text{B-3}$$

φ-component

$$\frac{\partial}{\partial t}\left(\rho_{g;TCE,N_2,water}\mathbf{v}_{\varphi_{g;TCE,N_2,water}}\right)+\mathbf{v}_{r_{g;TCE,N_2,water}}\frac{\partial}{\partial r}\left(\rho_{g;TCE,N_2,water}\mathbf{v}_{\varphi_{g;TCE,N_2,water}}\right)$$
$$+\frac{\mathbf{v}_{\varphi_{g;TCE,N_2,water}}}{r}\frac{\partial}{\partial\varphi}\left(\rho_{g;TCE,N_2,water}\mathbf{v}_{\varphi_{g;TCE,N_2,water}}\right)+\frac{\mathbf{v}_{r_{g;TCE,N_2,water}}\mathbf{v}_{\varphi_{g;TCE,N_2,water}}}{r}$$
$$+\mathbf{v}_{z_{g;TCE,N_2,water}}\frac{\partial}{\partial z}\left(\rho_{g;TCE,N_2,water}\mathbf{v}_{\varphi_{g;TCE,N_2,water}}\right)=\frac{\rho_{g;TCE,N_2,water}g}{\eta\theta_{g;TCE,N_2,water}}$$
$$-\frac{1}{\eta\theta_{g;TCE,N_2,water}}\left\{\frac{1}{r}\frac{\partial P_{\varphi_{g;TCE,N_2,water}}}{\partial\varphi}\right\}$$
$$+\mu_{g;TCE,N_2,water}\eta\theta_{g;TCE,N_2,water}\left\{\frac{\partial^2\mathbf{v}_{\varphi_{g;TCE,N_2,water}}}{\partial r^2}\right.$$
$$-\left(\frac{\mathbf{v}_{\varphi_{g;TCE,N_2,water}}}{r^2}\right)+\frac{\partial\mathbf{v}_{\varphi_{g;TCE,N_2,water}}}{\partial r}+\frac{2}{r^2}\frac{\partial^2\mathbf{v}_{\varphi_{g;TCE,N_2,water}}}{\partial\varphi^2}$$
$$\left.+\frac{2}{r^2}\frac{\partial\mathbf{v}_{r_{g;TCE,N_2,water}}}{\partial\varphi}+\frac{\partial^2\mathbf{v}_{\varphi_{g;TCE,N_2,water}}}{\partial z^2}-\frac{2}{3r}\frac{\partial}{\partial\varphi}\left(\nabla\cdot\mathbf{v}_{g;TCE,N_2,water}\right)\right\}$$

B-4

z-component

$$\frac{\partial}{\partial t}\left(\rho_{g;TCE,N_2,water}\mathbf{v}_{z_{g;TCE,N_2,water}}\right)+\mathbf{v}_{r_{g;TCE,N_2,water}}\frac{\partial}{\partial r}\left(\rho_{g;TCE,N_2,water}\mathbf{v}_{z_{g;TCE,N_2,water}}\right)$$
$$+\frac{\mathbf{v}_{\varphi_{g;TCE,N_2,water}}}{r}\frac{\partial}{\partial\varphi}\left(\rho_{g;TCE,N_2,water}\mathbf{v}_{z_{g;TCE,N_2,water}}\right)+\mathbf{v}_{z_{g;TCE,N_2,water}}\frac{\partial}{\partial z}\left(\rho_{g;TCE,N_2,water}\mathbf{v}_{z_{g;TCE,N_2,water}}\right)$$
$$=\frac{\rho_{g;TCE,N_2,water}g}{\eta\theta_{g;TCE,N_2,water}}-\frac{1}{\eta\theta_{g;TCE,N_2,water}}\left\{\frac{\partial P_{z_{g;TCE,N_2,water}}}{\partial z}\right\}$$
$$+\mu_{g;TCE,N_2,water}\eta\theta_{g;TCE,N_2,water}\left\{\frac{1}{r}\frac{\partial}{\partial r}\left(r\frac{\partial\mathbf{v}_{z_{g;TCE,N_2,water}}}{\partial r}\right)+\frac{1}{r^2}\frac{\partial^2\mathbf{v}_{z_{g;TCE,N_2,water}}}{\partial\varphi^2}\right.$$
$$\left.+\frac{\partial^2\mathbf{v}_{z_{g;TCE,N_2,water}}}{\partial z^2}-\frac{2}{3}\frac{\partial}{\partial z}\left(\nabla\cdot\mathbf{v}_{g;TCE,N_2,water}\right)\right\}$$

B-5

Conservation of Energy

(gas phase)

$$\frac{\partial}{\partial t}\left(\boldsymbol{\rho}_{g;TCE,N_2,water}\hat{\mathrm{U}}_{g;TCE,N_2,water}\right)$$
$$=-\left(\nabla\cdot\rho_{g;TCE,N_2,water}\mathbf{v}_{g;TCE,N_2,water}\hat{\mathrm{U}}_{g;TCE,N_2,water}\right) \qquad \text{B-6}$$
$$-\left(k\nabla^2\mathrm{T}\right)-\left(\nabla\cdot\mathrm{P}\mathbf{v}_{g;TCE,N_2,water}\right)+\mathrm{Q}$$

(liquid phase)

$$\frac{\partial}{\partial t}\left(\boldsymbol{\rho}_{l;TCE,N_2,water}\hat{\mathrm{U}}_{l;TCE,N_2,water}\right)=-\left(k\nabla^2\mathrm{T}\right)+\mathrm{Q} \qquad \text{B-7}$$

REFERENCES

Abriola, L. M., & Pinder, G. F. (1985a). A multiphase approach to the modeling of porous media contamination by organic compons, 1, equation development. *Water Resources Research, 24*(1), 11-18.

Abriola, L. M., & Pinder, G. F. (1985b). A multiphase approach to the modeling of porous media contamination by organic compounds, 2, numerical simulation. *Water Resources Research, 21*(1), 19-26.

Adenekan, A. E., Patzek, T. W., & Pruess, K. (1993). Modeling of multiphase transport of multicomponent organic contaminants and heat in the subsurface - numerical-model formulation. *Water Resources Research, 29*(11), 3727-3740.

Acierno, D., Barba, A. A., d'Amore, M., Pinto, I. M., & Fiumara, V. (2004). Microwaves in soil remediation from vocs. 2. Buildup of a dedicated device. *Aiche Journal, 50*(3), 722-732.

Acierno, D., Barba, A. A., and d'Amore, M. (2003). Microwaves in soil remediation from VOCs. 1: Heat and mass transfer aspects. *AIChE Journal, 49*(7), 1909-1921.

Agency for Toxic Substances and Disease Registry (2003). *ToxFAQs for Trichloroethylene.* (United States Department of Health and Human Services, Public Health Service). Atlanta, Georgia.

Agency for Toxic Substances and Disease Registry (2002). *Fiscal year 2002 Agency Profile and Annual Report October 1, 2001, to September 30, 2002* (United States Department of Health and Human Services, Public Health Service). Atlanta, Georgia.

Benard, J., Eymard, R., Nicolas, X., and Chavant, C. (2005). Boiling in porous media: Model and simulations. *Transport in Porous Media, 60*(1), 1-31.

Beyke, G., and Flemming, D. (2005). *In situ* thermal remediation of DNAPL and LNAPL using electrical resistance heating. *Remediation, 15*(3), 5-22.

Bird, R. B., Stewart, W. E., and Lightfoot, E. N. (1960). *Transport phenomena*. New York: John Wiley & Sons.

Bridges, J., Snow, R., and Taflove, A. (1979). Method for *in-situ* processing of hydrocarbonaceous formations. *U.S. Patent No.* 4,140,180. Washington DC: U.S. Patent and Trademark Office.

Buettner, H. M., and Daily, W. D. (1995). Cleaning contaminated soil using electrical heating and air stripping. *Journal of Environmental Engineering-ASCE, 121*(8), 580-589.

Carrigan, C. R., & Nitao, J. J. (2000). Predictive and diagnostic simulation of in situ electrical heating in contaminated, low-permeability soils. *Environmental Science & Technology, 34*(22), 4835-4841.

Chute, F. S., and Vermeulen, F. E. (1988). Present and potential applications of electromagnetic heating in the *in-situ* recovery of oil. *AOSTRA Journal of Research, 4*(1), 19-33.

CRC handbook of chemistry and physics (1990). 71st Ed., D.R. Lide, ed. in chief. Boca Raton: CRC Press.

Dablow III, J. F., Johnson, P. C., and Pearce, J. A. (2000). *Steam and electroheating remediation of tight soils*. New York: Lewis Publishers.

Daniel, D. E., Loehr, R. C., Webster, M. T., and Kasevich, R. S. (2000). *Soil vapor extraction using radio frequency heating*. New York: Lewis Publishers.

Davis, E.L. United States Environmental Protection Agency. (1998). Steam injection for soil and aquifer remediation (EPA Office of Research and Development, report #EPA/540/S-97/505). Research Triangle Park, North Carolina.

Davis, E.L. United States Environmental Protection Agency. (1997). How heat can enhance in-situ soil and aquifer remediation: important chemical properties and guidance on choosing the appropriate technique (EPA Office of Office of Research and Development, Office of Solid Waste and Emergency Response, report #EPA/540/S-97/502). Research Triangle Park, North Carolina.

Dev, H. (1993). Management plan: Demonstration testing and evaluation of in situ soil heating. *U.S. Department of Energy Contract Number* DE-AC05-930R22160.

Dev, H., Enk, J., Sresty, G., Bridges, J., & Downey, D. (1989). *In-situ* decontamination by radio-frequency heating - field test. *U.S. Air Force Contract No.* F04701-86-C-0002: Los Angelos, CA.

Di, P., Chang, D. P. Y., and Dwyer, H. A. (2002). Modeling of polychlorinated biphenyl removal from contaminated soil using steam. *Environmental Science & Technology, 36*(8), 1845-1850.

Dwyer, A. S., Kasevich, R. S., and Myer, K. (1979). *In-situ* radio frequency selective heating process; Petroleum products from kergoen in oil shale formations. *U.S. Patent No*. 4,140,179. Washington DC: U.S. Patent and Trademark Office.

Edelstein, W. A., Iben, I. E. T., Mueller, O. M., Uzgiris, E. E., Philipp, H. R., and Roemer, P. B. (1994). Radiofrequency ground heating for soil remediation - science and engineering. *Environmental Progress, 13*(4), 247-252.

Falta, R. W., Pruess, K., Javandel, I., & Witherspoon, P. A. (1992). Numerical modeling of steam injection for the removal of nonaqueous phase liquids from the subsurface.1. Numerical formulation. *Water Resources Research, 28*(2), 433-449.

Heine, K. S., and Steckler, D. J. (1999). Augmenting in-situ remediation by soil vapor extraction with six-phase soil heating. *Remediation*, 65-72.

Heron, G., Van Zutphen, M., Christensen, T. H., & Enfield, C. G. (1998). Soil heating for enhanced remediation of chlorinated solvents: A laboratory study on resistive heating and vapor extraction in a silty, low-permeable soil contaminated with trichloroethylene. *Environmental Science & Technology, 32*(10), 1474-1481.

Jones, D. A., Lelyveld, T. P., Mavrofidis, S. D., Kingman, S. W., and Miles, N. J. (2002). Microwave heating applications in enviromnental engineering - a review. *Resources Conservation And Recycling, 34*(2), 75-90.

Kawala, Z., and Atamanczuk, T. (1998). Microwave enhanced thermal decontamination of soil. *Environmental Science & Technology, 32*(17), 2602-2607.

Poppendieck, D. G., Loehr, R. C., and Webster, M. T. (1999). Predicting hydrocarbon removal from thermally enhanced soil vapor extraction systems 1. Laboratory studies. *Journal of Hazardous Materials*, 81-93.

Price, S. L., Kasevich, R. S., Johnson, M. A., Wiberg, D., and Marley, M. C. (1999). Radio frequency heating for soil remediation. *Journal of the Air & Waste Management Association, 49*(2), 136-145.

Pruess, K. (1983). Development of the general purpose simulator MULKOM. Earth Sciences Division Annual Report 1982, *Rep. LBL-15500*, Lawerence Livermore National Laboratory: Berkeley, California.

Pruess, K. (1987). Tough user's guide. *Rep. NUCREG/CR-4645,* Nuclear Regulatory Commission*: Wasington, D.C.*

Schwarzenbach, R. P., Gschwend, P. M., and Imboden, D. M. (1993). *Environmental organic chemistry*. New York: Wiley & Sons.

Sleep, B. E., and Ma, Y. F. (1997). Thermal variation of organic fluid properties and impact on thermal remediation feasibility. *Journal of Soil Contamination, 6*(3), 281-306.

Sresty, G. C. (1994). Treatability study work plan, Demonstration testing and evaluation of in situ soil heating. *U.S. Department of Energy Contract* DE-AC05-930R22160.

United States Environmental Protection Agency. (1997). Analysis of selected enhancements for soil vapor extraction (EPA Office of Solid Waste and Emergency Response, report #EPA/542-R-97-007). Research Triangle Park, North Carolina.

United States Environmental Protection Agency. (2004). *In situ* thermal treatment of chlorinated solvents (EPA Office of Solid Waste and Emergency Response, report #EPA/542-R-04-0100). Research Triangle Park, North Carolina.

United States Environmental Protection Agency. (1994). How to evaluate alternative cleanup technologies for underground storage tank sites: A guide for corrective action plan reviewers (EPA Office of Solid Waste and Emergency Response, report # EPA/510-R-04-002). Research Triangle Park, North Carolina.

Van Deuren, J., Lloyd, T., Chhetry, S., Liou, R., and Peck, J. (2002). Remediation technologies screening matrix and reference guide, 4th edition. Federal Remediation Technologies Roundtable. Retrieved February 22, 2006 from http://www.frtr.gov/matrix2/top_page.html